Cell

Paleogenomes reveal the evolutionary relationship between modern and cave lions

Graphical abstract

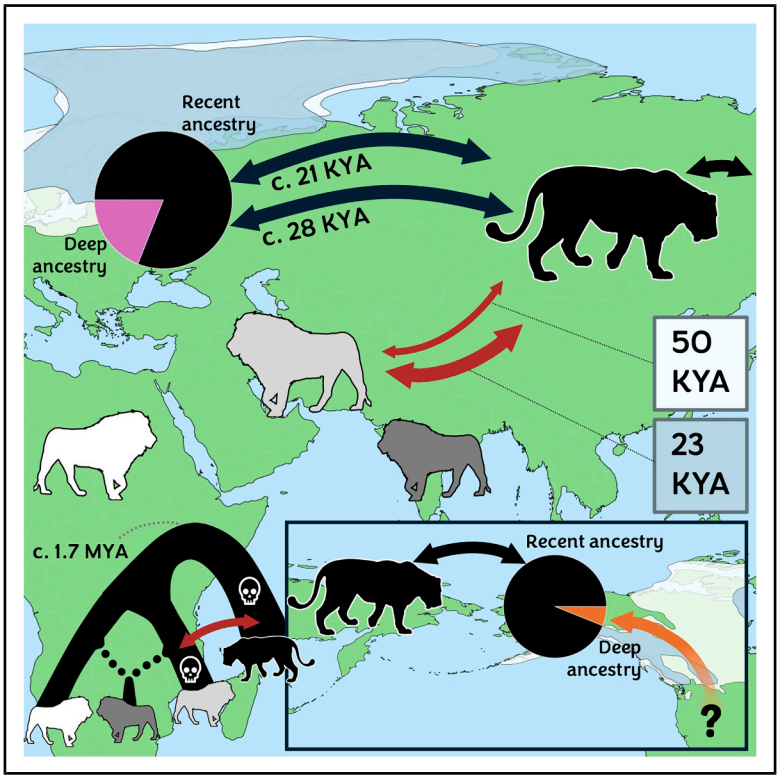

Highlights

- Cave and modern lions were distinct evolutionary lineages with independent histories
- Cave lions possessed many unique functional mutations across the genome
- Gene flow occurred between modern and cave lions during the Late Pleistocene
- Cave lions were highly connected across their distribution

Authors

David W.G. Stanton, Anders Bergström, Peter D. Heintzman, ..., Pontus Skoglund, Laurent Frantz, Love Dalén

Correspondence

stantondw@cardiff.ac.uk (D.W.G.S.), love.dalen@zoologi.su.se (L.D.)

In brief

Paleogenomic analysis of cave lions spanning >100 kya shows that extinct cave lions formed a long-diverged evolutionary lineage from modern lions, with distinct demographic histories and lineage-specific functional variation. Evidence of Late Pleistocene gene flow between cave and modern lions provides insight into the ecology and extinction dynamics of one of the Northern Hemisphere's most influential megafaunal predators.

Stanton et al., 2026, Cell *189*, 1–12
July 9, 2026
https://doi.org/10.1016/j.cell.2026.05.007

CellPress

Cell

CellPress
OPEN ACCESS

Article

Paleogenomes reveal the evolutionary relationship between modern and cave lions

David W.G. Stanton,[1,2,3,4,30,*] Anders Bergström,[5,6] Peter D. Heintzman,[3,7] Tom van der Valk,[3,4] Alberto Carmagnini,[8] Erik Ersmark,[3,4] Harvinder Pawar,[9] Marcela Sandoval-Velasco,[10,11] Semyon Androsov,[12] Sergey Fedorov,[13] Martin Kuhlwilm,[9,14,15] Doris Nagel,[15,16] Valeri Plotnikov,[17] Albert Protopopov,[17] Beth Shapiro,[18,19] Ross Barnett,[20] Mikkel-Holger S. Sinding,[10,21] Tomas Marques-Bonet,[9,22,23,24] Nobuyuki Yamaguchi,[25,26] M. Thomas P. Gilbert,[10,27] Anders Götherström,[3,28] Pontus Skoglund,[6] Laurent Frantz,[2,8] and Love Dalén[3,4,29,*]

[1]Cardiff School of Biosciences, Sir Martin Evans Building, Cardiff University, Museum Avenue, Cardiff CF10 3AX, UK
[2]School of Biological and Behavioural Sciences, Queen Mary University of London, London, UK
[3]Centre for Palaeogenetics, Svante Arrhenius väg 20C, 106 91 Stockholm, Sweden
[4]Department of Bioinformatics and Genetics, Swedish Museum of Natural History, Stockholm, Sweden
[5]School of Biological Sciences, University of East Anglia, Norwich, UK
[6]Ancient Genomics Laboratory, The Francis Crick Institute, London, UK
[7]Department of Geological Sciences, Stockholm University, 106 91 Stockholm, Sweden
[8]Chair of Animal Systems Genomics, Faculty of Veterinary Medicine, Ludwig-Maximilians-Universität, Munich, Germany
[9]Institute of Evolutionary Biology (UPF-CSIC), PRBB, Dr. Aiguader 88, 08003 Barcelona, Spain
[10]The GLOBE Institute, Faculty of Health and Medical Sciences, University of Copenhagen, Øster Farimagsgade 5A, 1353 Copenhagen, Denmark
[11]Centro de Ciencias Genómicas, Universidad Nacional Autónoma de México, Cuernavaca, Morelos, Mexico
[12]Museum "Severnyi Mir", Yakutsk, Sakha Republic (Yakutia), Russia
[13]Mammoth Museum of North-Eastern Federal University, Yakutsk, Sakha Republic (Yakutia), Russia
[14]Department of Evolutionary Anthropology, University of Vienna, Djerassiplatz 1, 1030 Vienna, Austria
[15]Human Evolution and Archaeological Sciences (HEAS), University of Vienna, Vienna, Austria
[16]Department of Paleontology, University of Vienna, Josef-Holaubek Platz 2, 1090 Vienna, Austria
[17]Academy of Sciences of Sakha Republic, Lenin Avenue 33, Yakutsk, Sakha Republic (Yakutia), Russia
[18]Department of Ecology and Evolutionary Biology, University of California, Santa Cruz, Santa Cruz, CA 95064, USA
[19]Colossal Biosciences, 1401 Lavaca St, Unit #155, Austin, TX 78701, USA
[20]Center for Evolutionary Hologenomics, The GLOBE Institute, University of Copenhagen, Copenhagen, Denmark
[21]Department of Birds and Mammals, Greenland Institute of Natural Resources, Nuuk, Greenland, Denmark
[22]Catalan Institution of Research and Advanced Studies (ICREA), Passeig de Lluís Companys, 23, 08010 Barcelona, Spain
[23]CNAG, Centro Nacional de Analisis Genomico, Baldiri i Reixac 4, 08028 Barcelona, Spain
[24]Institut Català de Paleontologia Miquel Crusafont, Universitat Autònoma de Barcelona, Edifici ICTA-ICP, c/ Columnes s/n, Cerdanyola del Vallès, Barcelona 08193, Spain
[25]Department of Zoology, Hungarian Natural History Museum, Baross Utca 13, Budapest 1088, Hungary
[26]Wildlife Conservation Research Unit, Department of Biology, University of Oxford, Life and Mind Building, South Parks Road, Oxford OX1 3EL, UK
[27]University Museum NTNU, Trondheim, Norway
[28]Department of Archaeology and Classical Studies, Stockholm University, 10691 Stockholm, Sweden
[29]Department of Zoology, Stockholm University, 10691 Stockholm, Sweden
[30]Lead contact
*Correspondence: stantondw@cardiff.ac.uk (D.W.G.S.), love.dalen@zoologi.su.se (L.D.)
https://doi.org/10.1016/j.cell.2026.05.007

SUMMARY

The Eurasian cave lion was abundant across the Northern Hemisphere before the Late Pleistocene megafaunal extinctions. However, the extent of the distinction between cave and modern lions and their adaptive differences have remained unclear. Using 12 cave lion genomes spanning more than 100,000 years, we show that modern and cave lions were distinct evolutionary lineages with separate demographic histories and unique non-synonymous variants. We also identify evidence of ancient gene flow between them, with the best modern lion proxy for this ancestry being an extinct Southwest Asian population. This admixture correlates with global ice extent, with 3.2%–4.4% modern lion ancestry detected in a ~20,000-year-old cave lion from Central East Asia. These findings provide insight into the evolutionary history of the cave lion, once one of the Northern Hemisphere's most ecologically impactful megafaunal species.

Please cite this article in press as: Stanton et al., Paleogenomes reveal the evolutionary relationship between modern and cave lions, Cell (2026), https://doi.org/10.1016/j.cell.2026.05.007

INTRODUCTION

Lions are among the most abundant and widespread mega-carnivores in the fossil record of the last c. 1 million years, with fossils found across four continents, including Africa, Europe, Asia, and the Americas at least as far south as Mexico.[1–3] The first fossils with clear lion characteristics appear in East Africa from c. 1.9 million years ago (mya),[4] and outside Africa by c. 1 mya, in El Kowm, Syria.[5] They are represented in the fossil record in Europe (Italy and England) from c. 700 thousand years ago (kya)[6–8] and in North America from c. 300 ka,[9] reaching the southern parts of North America (American lion, *Panthera atrox*), and potentially even South America, from c. 130 ka.[10] Lions are currently restricted to a single, small population in India and fragmented populations in Africa (*Panthera leo*, hereafter referred to as "modern lions"). Evidence from skeletal remains, preserved soft tissue, and Pleistocene cave art indicates that extinct Late Pleistocene lions from the Northern Holarctic (*Panthera spelaea*, hereafter referred to as "cave lions") were morphologically distinct from modern lions. They were larger than their modern counterparts[6,11] and probably had lighter hair.[10] Stable isotope results, interpreted as evidence for an individualistic diet,[12] and Paleolithic art indicating that male cave lions lacked manes (or that they were considerably reduced),[11] have been used to suggest that, unlike modern lions, cave lions were likely to be predominantly solitary, although this has been disputed.[3,13] This distinction is also reflected at a genetic level, demonstrating that modern lions and cave lions were distinct species based on extensive mitochondrial sampling and nuclear DNA from a small number of specimens.[14–17] Lions have been estimated to have diverged from their closest extant relative, the leopard (*Panthera pardus*), c. 2.6 mya,[18] although due to complex admixture events, these divergence times are challenging to estimate precisely.[19] Divergence times between modern lions and cave lions have been estimated at c. 500 ka, based on nuclear genome data,[14] with American lions (*P. atrox*) constituting a sister lineage to cave lions. However, estimates based on mitochondrial genomes and fossil constraints suggest the divergence may be considerably older (up to 1.9 mya).[16,17] Also, the extent to which this genome-wide distinction holds across space and time is not known. Fossil evidence suggests that cave lions showed extensive temporal and spatial variation in morphology,[20] with serial replacement by discrete forms of decreasing size throughout the Pleistocene.[21] Given the extensive historic distribution of cave lions, if this continuous replacement was occurring, it would imply substantial connectivity between lions over vast geographic areas, a process that has been suggested to have occurred from East to West.[22] In contrast to the proposed high levels of connectivity, it has also been hypothesized that gene flow may have been periodically restricted between Eastern and Western Eurasia, with the expansion of water bodies northward (in particular the Caspian Sea, glacial lakes, and the Aral Sea) and ice sheets southward being proposed as factors that would have reduced, or even stopped, gene flow between Eastern Eurasia and Europe.[23] In addition, population replacements may not have been synchronous across the species' range, with ancestral size morphs being identified in more recent contexts, in particular in Europe,[20–22] suggesting that this may have been a refugium for a more ancestral lineage. Moreover, gaps in cave lion ^{14}C dates might reflect local extirpation from Europe for several thousand years during the Late Pleistocene, prior to their range-wide terminal extinction.[11] At the eastern side of the distribution, it seems highly probable, based on the dispersal patterns of other large mammals,[24,25] that the Bering Strait and land bridge would have led to intermittent isolation and connectivity, respectively, between c. 70 and 11 ka.[26] Together, these data suggest the possibility of geographically and temporally restricted lineages and extinctions, hypotheses that would not be possible to test with existing datasets.

Despite its commonness in the Holarctic fossil record throughout much of the later Pleistocene, the cave lion appears to have gone extinct more or less synchronously across its entire range, with terminal fossil dates of between c. 14 and 13 ka.[11] The cave lion lineage therefore forms part of the global megafaunal extinctions that occurred during the last glacial-interglacial transition, and it precedes the extinction of many of the mega-herbivores.[4,27] Modern lion populations have also likely declined since the Late Pleistocene,[28] exacerbated more recently due to anthropogenic factors[29,30] and ultimately leading to the extinction of "Barbary lions" (North Africa), "Cape lions" (South Africa), and "Mesopotamian lions" (Southwest Asia).[14] The extinction of cave lions probably had a disproportionately large ecological effect across the Holarctic. Mega-carnivores ($\geq$100 kg) can have top-down effects on ecosystems by regulating the abundance and activity of large herbivores, either through direct consumption or by inducing indirect behavioral changes.[28,31] Their abundance and wide distribution make it likely that lions in particular would have had a considerable influence on their ecosystem, including the evolution of other sympatric carnivores,[32,33] although the complexity and interconnectedness of these ecosystems makes inferring the outcome of any given species extinction extremely difficult.[34]

Cave lions are thought to have been distributed as far south as the Caucasus, eastern Turkey, southern Siberia, and Manchuria, and contact zones have been proposed with modern lions in South-East Europe and/or the Caucasus.[1,2] It has been argued that modern lions only entered the former distribution range of cave lions after they had gone extinct,[11] and previous studies have not found any evidence for gene flow.[1,14,35] However, these studies have either focused on mitochondrial DNA[1,35] or relied on two cave lion nuclear genomes, both from Beringia and of approximately the same age. This is over 5,000 km away from the range of modern lions and any proposed contact zones,[14] leaving open the possibility of admixture between modern lions and cave lions at different time points and/or locations. The plausibility of this hypothesis is increased by the fact that felids have a known history of extensive introgression, with ancient hybridization events having been detected across multiple taxonomic groups, including those more distantly related than modern lions and cave lions.[18,19,36,37] Also, mismatches between cave lion sample locations and sizes have led to the hypothesis that historic glacial cycles may have caused distribution shifts in cave lions, for example, the range shifting southward during increased ice extent.[21]

Considering their important ecological role as a widely distributed apex predator, lions present an opportunity to better

Please cite this article in press as: Stanton et al., Paleogenomes reveal the evolutionary relationship between modern and cave lions, Cell (2026), https://doi.org/10.1016/j.cell.2026.05.007

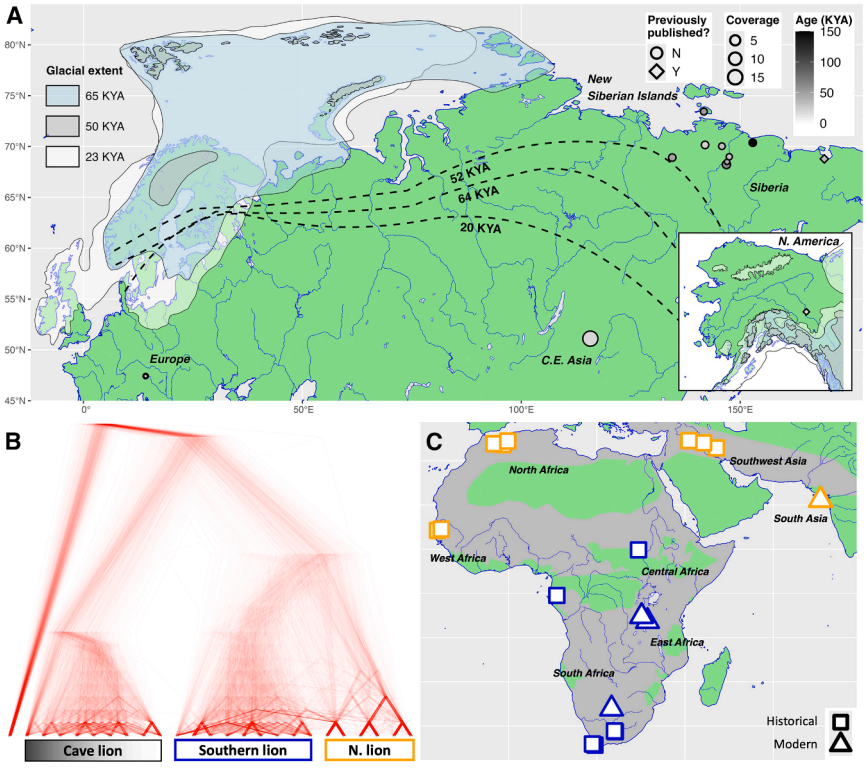

Figure 1. Cave and modern lion sample distribution and phylogenetic structure

(A) Eurasia (main) and North America (inset), with points showing cave lion genomes used in the present study (Table S1). Estimated age is shown by color scale (darker = older), new/existing data are shown by shape (circles are newly generated genomes), and genome coverage is denoted by shape size. Approximate glacial and tundra biome extents at various time periods are shown by polygons and dashed lines, respectively, based on Huntley et al.[39] Key samples referred to in the text are "Yukon_33KYA" (N. America), "Austria_17KYA" (Europe), "CE_Asia_20KYA" (C.E. Asia), and "NSI_52KYA" (New Siberian Islands).

(B) DensiTree[40] phylogeny created (using RAxML[41] on 2 MB non-overlapping windows) for all >1× lion genomes from Table S1. >99% of RAxML phylogenies placed modern and cave lions into monophyletic clades. The cave lion and southern and northern modern lion lineages are shown in grayscale, blue, and orange, respectively, with corresponding colors on the maps.

(C) Modern lion genomes included in the present study (Table S1). Pleo_Captive1 and Pleo_Captive2 are not shown on the map due to uncertain provenance. Shapes correspond to sample age. Gray shading shows the putative historical species distribution,[42] with southern and northern modern lion lineages shown in blue and orange, respectively, with corresponding colors on the phylogeny.

understand how long-term climatic changes influence evolutionary processes over large geographic scales. In the present study, we sequenced genomes of cave lions across a time series spanning over 100,000 years to test whether modern and cave lions are monophyletic throughout the Upper Middle Pleistocene and Late Pleistocene, across their entire distribution. In addition, we investigate inter- and intraspecific connectivity across an extensive spatiotemporal scale. Together, these tests aim to describe the broadscale evolutionary processes, namely population structure and introgressive history, acting on this widespread mega-carnivore in the lead-up to the extinction of what would have been one of Pleistocene Eurasia's most ecologically important megafaunal species.

RESULTS AND DISCUSSION

Samples and sequencing

We generated whole-genome sequences from 10 cave lion samples, following an initial screening of 52 specimens. Mean coverage of these samples was 3.5× (min 0.3×, max 19.5×). We radiocarbon dated one sample that had not been dated previously and used mitochondrial tip-dating[17] to estimate the ages of samples with non-finite ^{14}C dates (n = 4; Table S1).

We also sequenced a museum specimen of one historic lion from the now-extinct Southwest Asian population. This individual was included here with the aim of confirming its provenance and incorporating an additional sample that would be informative about modern/cave lion gene flow (contingent on provenance). We combined these genomes with 2 cave lion and 20 modern lion genomes that had previously been published,[14] along with 6 outgroup species (Amur leopard,[38] snow leopard, Bengal and Siberian tigers,[38] jaguar,[18] and mainland clouded leopard[14]) (Table S1). The cave lion samples constitute a time series spanning c. 148–17 ka and come from a geographic distribution spanning central Europe (Austria; "Austria_17KYA") to North America (Yukon; "Yukon_33KYA") and South-Central Asia.

Population structure

The Felidae phylogeny has been notoriously difficult to characterize, even with whole-genome data, due to historic hybridization events that can lead to discordant phylogenetic patterns across the genome.[19,36] It is therefore possible that a genome-wide phylogenetic assessment (as has previously been carried out) is not representative of the species tree. An assessment of the lion phylogeny across the genome would thereby give additional support to the conclusion that modern and cave lions constitute distinct species.

We investigated this using phylogenetic (TreeMix and a maximum-likelihood, sliding-window approach) and f-statistic-based analyses to describe genetic structure in lions across their current and historic distribution. Both phylogenetic analyses identify cave lions and modern lions to be reciprocally monophyletic across their genomes (>99% of maximum-likelihood phylogenies for 500 kb, 1 Mb, and 2 Mb sliding windows) and modern lions to be separated into southern/eastern ("southern modern lions") and northern/western ("northern modern lions") clades (Figure 1B). These results support previous observations based on

Please cite this article in press as: Stanton et al., Paleogenomes reveal the evolutionary relationship between modern and cave lions, Cell (2026), https://doi.org/10.1016/j.cell.2026.05.007

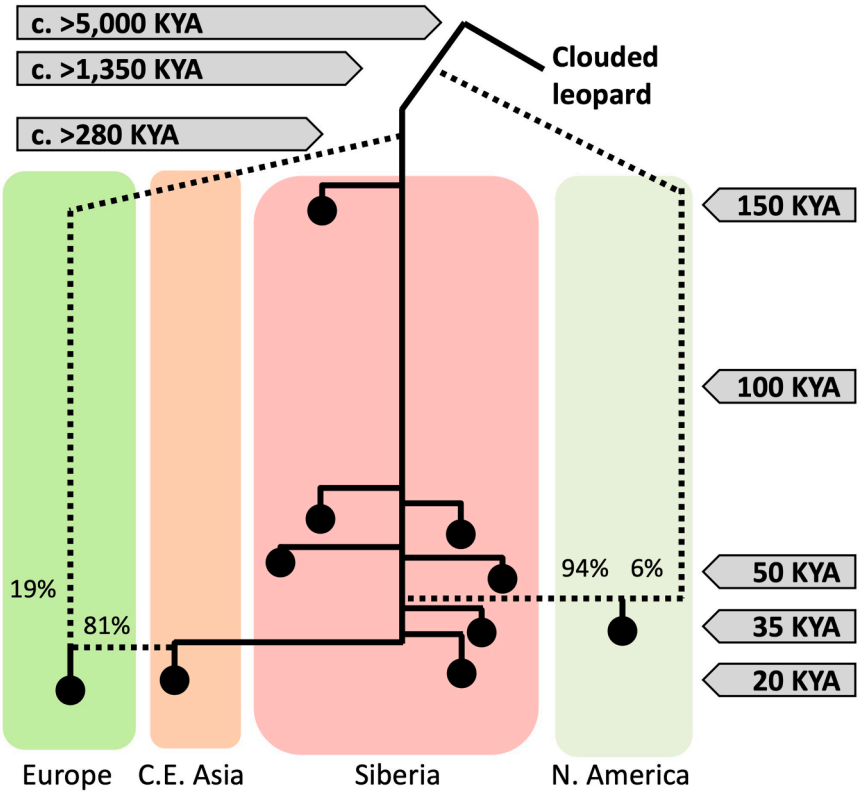

Figure 2. Admixture graph summarizing cave lion genetic structure, approximate divergence times, and admixture events
See also Figure S5H.

mitochondrial[1,17,43] and nuclear[14] data that modern and cave lions are distinct lineages. In addition, the European cave lion genome was basal to the other cave lion genomes in <5% of trees (for all sliding-window sizes), providing no support for a distinct lineage in Europe. The modern lion genomes of presumed Southwest Asian origin grouped together to the exclusion of all other modern lions (based on TreeMix analysis, and admixture graph topology strongly supported ($p < 0.001$) compared with any topology where these three Mesopotamian lions were not in a monophyletic clade; Figure S2), confirming their provenance as Southwest Asian. In addition, although the two captive but wild-born Indian lions (Gir Forest) cluster with the Northern modern lion lineage based on average genome-wide variation (TreeMix, Figures S2A and S2B), they show clear evidence for recent introgression of genomic tracts from the southern modern lion lineage (Figure 1B). It has previously been argued that the remaining Indian lion population, currently restricted to the Gir National Park, is not indigenous to the region but rather introduced from outside of India.[44,45] Previous publications have found no evidence for this claim.[14,46] These Indian lions were wild-born (Gir Forest) captive zoo animals, suggesting that there has been recent introgression into the wild Indian population from the southern modern lion lineage. Captive Asiatic lions are known to have been recently interbred with African lions, and our results suggest that either the two analyzed Indian lions were not in fact wild born or that genetic leakage has occurred from the Indian captive population into the wild Gir Forest population. Outgroup f3 analyses identified that shared genetic drift between recent cave lions (from Siberia [22 ka], Central East [C.E.] Asia [20 ka], and Europe [17 ka]) and all other genomes increases gradually over time. In addition, those three most recent genomes share more drift with each other than they do with earlier genomes (Figures S5A–S5C). This suggests geographically extensive ancestry connectivity in cave lions, similar to what has recently been observed in wolves.[25] The genome from North America (Yukon_33KYA) displays lower shared genetic drift with other contemporary genomes, in particular with the recent European cave lion (Figure S5A). This finding of genetic structure between Europe and North America is in line with a previous study of mitochondrial genomes suggesting that there is some genetic structure between Eastern and Western cave lions, with monophyletic clades being almost entirely segregated to the East and West (Beringia and North America vs. the rest of the range).[17]

To investigate the timing and extent of East-West connectivity further, we used f4 statistics to compare our time series of Siberian genomes with contemporaneous but geographically distant pairs of genomes. No genetic structure (i.e., non-significant f4 values) was detected across any spatial scale between C.E. Asia and Siberia, suggesting complete ancestry homogenization across this region. In contrast, Europe and North America both showed genetic structure with respect to Siberia, with at least some genetic structure persisting as far as the oldest Siberian genome sample (148 ka; Figure S5D). To investigate any differences in cave lion genetic structure between the eastern and western extents of their distribution, we used f4 statistics to compare genomes from North America and Europe to our time series of Siberian genomes. All comparisons show more shared ancestry between East and West Eurasia compared with East Eurasia and North America, again suggesting relatively high levels of gene flow across Eurasia (Figure S5E). The test does not distinguish between deep ancestry and recent structure that may be present in North America; however, all significant comparisons in this test ($n = 4$ of 10) are within the past 52 ka, indicating that more recent processes also had some impact on gene flow. Glacial cycles are thought to have been a driver of historic faunal connectivity/isolation, with the Bering Strait most likely to have last been open during the Eemian (c. 129 to 116 ka) but with subsequent periods of connectivity/isolation, especially between c. 70 and 11 ka.[26] Our results suggest that

Please cite this article in press as: Stanton et al., Paleogenomes reveal the evolutionary relationship between modern and cave lions, Cell (2026), https://doi.org/10.1016/j.cell.2026.05.007

these periods of isolation led to the accumulation of local structure in North American cave lions, potentially including ancestry originating from outside the cave lion clade that was not fully homogenized when connectivity was reestablished. Cave lion gene flow appears to have been extensive across Eurasia, being detected between Siberia and C.E. Asia, and Siberia and Europe, between 33 and 22 ka, and between C.E. Asia and Europe between 22 and 20 ka (Figures S5F and S5G). These shifts in ancestry differentiate cave lions that lived before compared with after those time periods and demonstrate that ancestry connectivity spans Eurasia and occurred over periods as short as c. 2 ka. Although additional older genomes would be required to test the direction of this gene flow, what is clear is that large-scale spatial connectivity occurred in cave lions, leading to homogenization of ancestry in large proportions of the genome, over relatively short periods. Previous research based on mitochondrial data has also identified East-West structuring in cave lions,[17] although, in that case, Eastern Eurasia and North America form a clade to the exclusion of Western Eurasia. Our results point to less ancestry shared between Eastern Eurasia and North America compared with Eastern Eurasia and Western Eurasia, although this finding is likely influenced by factors such as the depth and proportion of the "deep ancestry" present in the North American genome. These results in Eurasia are again similar to what has been seen in wolves, where a small amount of deep genetic structure persists for long (c. >100 ka) periods of time, but ancestry is otherwise consistently homogenized over relatively short timescales.

Gaps in cave lion ^{14}C dates indicate that the species may have gone locally extinct in Europe during the Last Glacial Maximum, before being recolonized from Siberia by approximately 18.5 ka.[11] If this, or other local extinctions, had occurred, they would have removed any deep, local ancestry present in that region. Therefore, to investigate the persistence of local genetic structure in Europe and North America, we used the qpWave/qpAdm modeling framework, using an outgroup (clouded leopard) as a proxy for unsampled deep ancestry. After validating that a multi-source model was indeed appropriate (qpWave, all single Siberian sources rejected at $p = 6.8e^{-7}$ and $p = 5.9e^{-52}$ for Europe and North America, respectively), we used qpAdm to estimate deep ancestry for the European and North American individuals (modeled as 4.7% [standard error (SE) = 0.9%] and 7.4% [SE = 0.7%], respectively, although the proportion is unconstrained when only using an outgroup). The C.E. Asian individual was modeled as having 0.0% deep ancestry (SE = 0.5%). Similar estimates were obtained in admixture graph analyses for the North American individual, which was best modeled with between 4% and 11% deep ancestry, whereas the European individual was modeled as having 10%–28% (Figures 2 and S5H). In these graph models, the deep ancestry detected in the European genome originates from a lineage that branched off relatively recently from our sampled cave lion diversity. Conversely, the deep ancestry detected in the North American individual originates from a point much further along the branch between our sampled cave lion diversity and the split between cave lions and clouded leopards (the split time between clouded leopard and lions is thought to be *at least* 5 mya based on both genetic and fossil evidence[47–49]). The deep European ancestry may therefore constitute an ancient, local cave lion origin, consistent with the outgroup source in the qpAdm model being a poor proxy, leading to a deflated value. In contrast, the deep ancestry in the North American genome appears more likely to have originated from some unknown source outside the cave lion clade, a situation remarkably similar to that seen in North American wolves (where this deep ancestry is explained by admixture with a sister canid lineage, such as the coyote[25] or red wolf).[50]

As mentioned above, we cannot rule out ghost introgression from a cryptic felid lineage in North American cave lions. A possible candidate for this ghost ancestry is the extinct American lion (*Panthera atrox*). American lions were characterized by a distribution in southern North America, extending as far south as Mexico,[3] with a specimen (c. 67 ka) recently being found in Yukon (North America), demonstrating that contact likely did occur.[51] To test our hypothesis that gene flow occurred between cave lions and *P. atrox*, we would need to sample and sequence from the *P. atrox* lineage. If the hypothesis were confirmed, it would represent a remarkable level of similarity in the population dynamics of cave lions and wolves, whereby ancestry is rapidly homogenized across their distribution, except for a component of deep ancestry remaining in genomes from North America and Europe. In North America this deep ancestry is consistent with introgression from a divergent lineage: coyotes or red wolves in the case of wolves and possibly an extinct American lion in the case of lions.

Gene flow with modern lions

To investigate potential instances of gene flow between different populations of modern lion and cave lion lineages, we used f4 statistics. Multiple, significant f4 statistics were consistent with instance(s) of gene flow between modern lions and cave lions (|Z|>3; *f4[Outgroup, Modern Lion-X; Cave-Y, Cave-Z]*), over the course of the last 150 ka (Figure S3). This gene flow appears to be at a low level (less than 5%) but with indications of temporal variability, whereby the highest estimates of modern lion ancestry are detectable in the cave lions aged 20, 22, and 64 ka (Figure 3A). This pattern was exemplified by a very clear difference when comparing the second-youngest specimen (a 20 ka individual from C.E. Asia) and the oldest specimen (a 148 ka individual from Yakutia), with 19 of the 21 comparisons in the same direction, indicating more shared drift between the younger cave lion and modern lions (*f4[Outgroup, Lion-X; CE_Asia_20KYA, Siberia_148KYA]*; Figure 3C), including all significant values ($z < -3$; 15 of 21 comparisons).

As the historic range of cave lions was geographically closer to northern (modern) lions than southern lions, we would expect (if the signal of gene flow were genuine) there to be a corresponding asymmetry in cave lion gene flow when comparing northern and southern modern lions. We assessed this asymmetry, and our confidence in it, using *Z* scores calculated from f-statistics of the type f4(Clouded leopard, Cave-X; Modern Lion1, Modern Lion2). This analysis consistently showed affinity between the cave lion individuals and the three modern lion individuals from Southwest Asia (Figures 4 and S4), which our results suggest belonged to the now-extinct Southwest Asian population (Figure S2C).

Please cite this article in press as: Stanton et al., Paleogenomes reveal the evolutionary relationship between modern and cave lions, Cell (2026), https://doi.org/10.1016/j.cell.2026.05.007

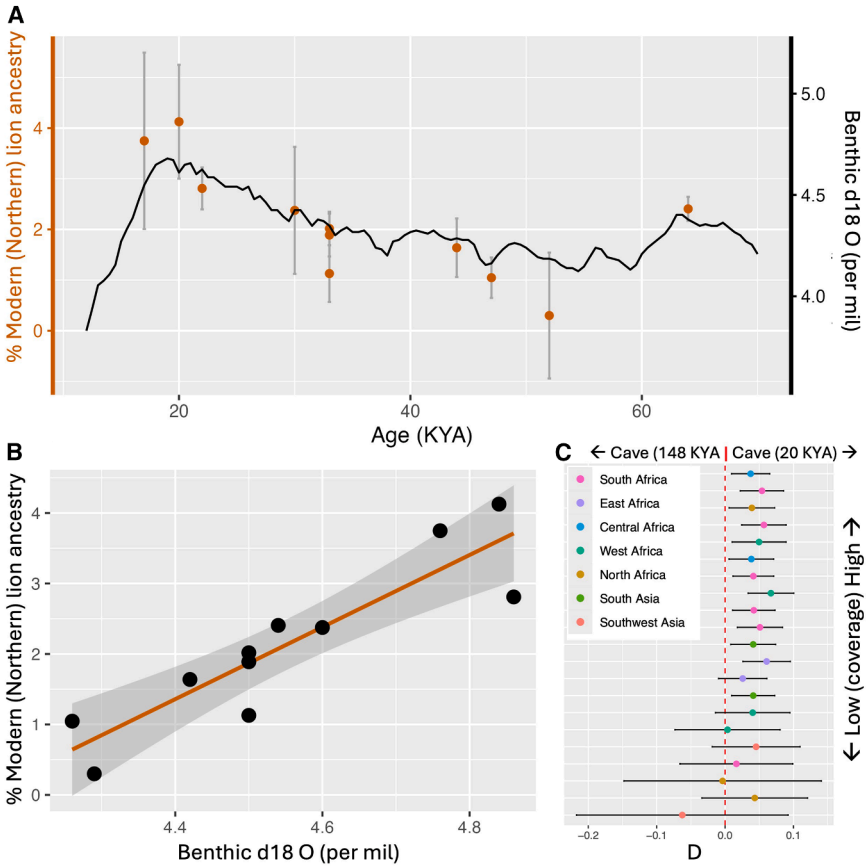

Figure 3. D-statistics and f4 ratios statistics to investigate gene flow asymmetries between cave lions and modern lions

(A) Percentage modern lion ancestry (mean alpha values from f4 ratio tests; *y* axis, red) for cave lions, with ages shown on the *x* axis. Benthic d18 O values are shown by a black line and on the alternative *y* axis. Values are given as averages for all combinations of high-coverage southern modern lion donor (Pop1) and northern modern lion donors (Pop5), with whiskers showing three SEs of the mean alpha for each cave lion.

(B) Correlation between percentage of modern lion ancestry in cave lion genomes and Benthic d18 O values (a proxy for global ice volume and deep ocean temperature).[51] Shaded area corresponds to 95% confidence interval.

(C) D-statistics comparing each modern lion to the 2nd youngest cave lion specimen (CE_Asia_20KYA) and the oldest cave lion specimen (Siberia_148KYA). Positive values show increased gene flow between that modern lion population (region shown by color) and the younger cave lion specimen relative to the older one. Error bars show 3 SEs.

See also Figure S3.

However, this association between introgression and time, exemplified by the comparison between the oldest and second-youngest cave lion genomes (Figure 3C), did not appear to hold for all cave lion individuals (Figure S3). To test this association further, we carried out f4-ratio tests to estimate the percentage of modern lion ancestry in cave lion genomes and modeled this as a function of Benthic d18 O levels, which is known to be a proxy for global ice volume and deep ocean temperature[52] (Figure 3). This revealed a strong correlation (R^2 = 0.808, $p = 1.7e^{-4}$), considerably higher than percentage modern lion ancestry vs. time (R^2 = 0.418, p = 0.032), although we could not reject the null hypothesis that these two correlations were equal (Steiger's Z test; z = 1.5969, p value = 0.1103). We hypothesize that historic increased ice extent has resulted in periods of increased modern-cave lion admixture. However, our earlier findings of homogenization, population structure, and deep ancestry demonstrate that there are likely additional conflicting evolutionary processes that would also influence this association. Notably, the North American cave lion genome, hypothesized to contain *P. atrox* ancestry, and the northernmost individual (New Siberian Islands), are the two specimens that show the largest negative deviation from the association (Figure 3). Taken together, these results suggest that, following the split between modern and cave lions, their isolation was punctuated by periods of contact and gene flow, likely driven by cyclical changes in climate during the Pleistocene. The times that we find the strongest evidence for this gene flow coincide with instances of higher-than-average global ice volume (based on $\delta^{18}O$ values[52]; Figure 3), presumably pushing the cave lion distribution southward, in line with our findings that the historic Southwest Asia modern lion genomes show the strongest affinity to cave lions. This affinity is stronger than that of North African and Western modern lions (the other lions in the Northern modern lion lineage; Figure 4), demonstrating that modern-cave lion gene flow occurred following the formation of population structure in Northern modern lions. However, multiple pulses of gene flow (Figure 3), and secondary admixture events between northern and southern modern lions following their divergence ~70,000 years ago,[14] likely contribute to the variable admixture patterns observed across different modern lion donors (Figures 3, S3, and S4). Modern lions are thought to have become established in Southwest Asia within the past 20 ka.[21,53,54] However, large herbivores would have been present in Central Asia during much of the Late Pleistocene, and our results indicate that lions were also present in this region, at least transiently, as early as 64,000 years ago, coinciding with periods of ice expansion (Figure 3). Introgression of this nature appears to be a feature of Pantherinae evolution, in line with previously detected interspecies gene flow across *Panthera* genomes.[18,19]

Lion demographic history

In order to investigate demographic history, we carried out a PSMC (pairwise sequentially Markovian coalescent) analysis (Figure 5A) on four high-coverage modern lion individuals from Southwest Asia, North Africa, and South Africa, as well as the one high-coverage cave lion individual (20 ka). We used a

Please cite this article in press as: Stanton et al., Paleogenomes reveal the evolutionary relationship between modern and cave lions, Cell (2026), https://doi.org/10.1016/j.cell.2026.05.007

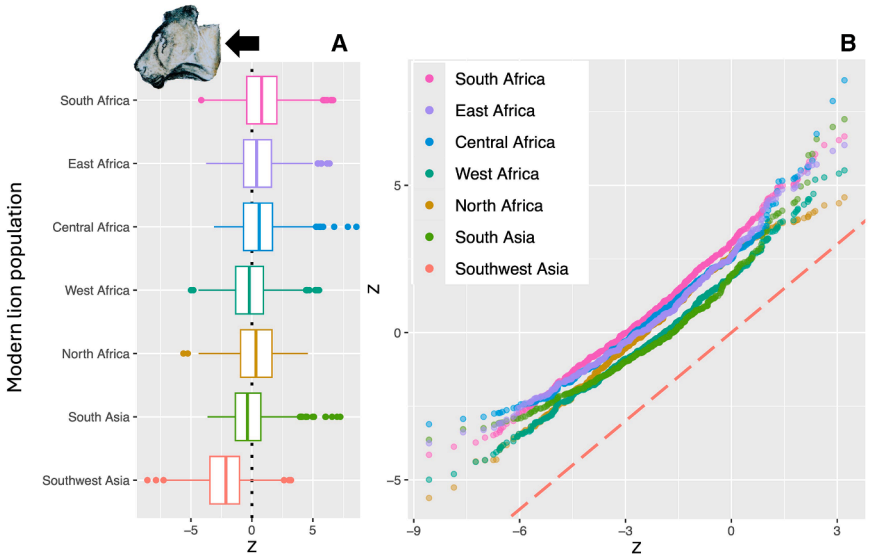

Figure 4. Investigation of asymmetry in gene flow between cave lions and the different modern lion populations

(A) Boxplots summarize the *Z* scores of f4 statistics for each of the cave lion samples compared with all combinations of the modern lion samples (see Figure S4), grouped by modern lion population (*y* axis). Left-shifted values indicate higher evidence for gene flow from cave lions into the named modern lion population on the *y* axis.

(B) QQ plot comparing the distributions of f4 statistic *Z* scores for comparisons involving each modern lion population (points; *y* axis quantiles), vs. the distribution for the comparisons involving the Southwest Asian lion (dashed line; *x* axis quantiles). Deviation of points from the dashed line indicates that the *Z* score distribution for other modern lion populations differs from that of the Southwest Asian lion, consistent with the stronger affinity between Southwest Asian lions and cave lions (as indicated by the direction and magnitude of *Z* scores in the left panel).

See also Figures S3 and S4.

mutation rate of $4.5e^{-9}$ and a generation time of 5 years, following de Manuel et al.[14] The cave and modern lion demographic histories started to diverge approximately 1 mya. Although the effective population size for cave lions was lower than that of modern lions throughout most of their independent demographic histories, the most recent N_e estimates for the cave lion are considerably higher than those of present-day modern lions. The Southwest Asian lion shows a divergent, and overall lower, effective population size relative to the other modern lion populations. Interestingly, as with the demographic histories of modern and cave lions, this appears to have started relatively early (c. 500 ka), predating the presumed divergence of the northern and southern modern lion lineages. Similarly ancient divergent demographic histories have previously been identified between different modern lion lineages (e.g., Northern and Central African),[14] suggesting that regional bottlenecks may have been acting on these lion lineages before they were fully separated.

The current best estimate of the divergence time for cave lions and modern lions is approximately 0.5 mya.[14] However, this divergence time is younger than expected, given that lion fossils are found in Syria by c. 1 mya,[5] and in Europe from c. 0.7 mya (Italy[8]; UK[7]), and considering divergence estimates of up to 1.9 mya based on mitochondrial genomes with fossil constraints.[16,17] Through simulations (Figure 5B), we were able to demonstrate that older divergence times are possible (including this upper-end estimate) once gene flow between cave and modern lions is accounted for. The highest density point of plausible values across all cave lion genomes occurred at a divergence time of 1.71 mya (342 K generations, assuming a generation time of 5 years), broadly in line with previous estimates based on mitochondrial sequences with fossil calibrations.[16,17] However, this analysis demonstrated that there were multiple viable combinations of divergence time and migration rate estimates between modern and cave lions that were consistent with our data. The estimate also depended on a variety of demographic factors, including (1) time since introgression, (2) extent of introgression (number of individuals), and (3) rate of cave lion ancestry turnover/replacement. Accurate determination of divergence time therefore requires separating out these contributory factors, which would be a valuable avenue for future research using increased temporal and spatial density of samples.

Unique protein-coding changes in cave lion genes

Despite the split between cave and modern lions having occurred relatively recently, it has been proposed that these lion lineages possess several differences relating to their morphology, behavior, and ecology, in particular body size,[6,11] males' mane,[13] and sociality.[11–13] Our dataset presents an opportunity to investigate functional genetic differences uniquely associated with the cave lion lineage.

After strict site filtering for depth, repeat elements, and missing data, we investigated 1.37 billion sites (58.8%) across six diploid outgroup individuals (Bengal tiger, Siberian tiger, mainland clouded leopard, jaguar, leopard, and snow leopard), 12 pseudohaploid cave lion individuals, and 21 pseudohaploid modern lion individuals. Across all genomes and variable positions (97.0 million), 0.54% (524,205) and 0.38% (371,538) of sites had alleles that were unique to, and fixed in, the cave lion individuals, respectively. Across all of the same individuals and variable positions (97.0 million), 26.3% (25.5 million) and 44.6% (43.3 million) of sites had alleles that were exclusive to the cave lion and modern lion lineages but not fixed within those lineages. To characterize the potential of this genetic variation to contribute to functional biological differences, we (1) carried out McDonald-Kreitman tests[55] to identify genes that had undergone strong positive selection in the cave lion lineage; (2) identified mutations predicted to have a high level of disruptive protein impact that were fixed in, and exclusive to, the cave lion lineage (using SnpEff[56,57]); and (3) carried out a test to identify genes with an excess of *de novo* (exclusive to cave lions relative to other felids), non-synonymous mutations in cave lions. Such genes could constitute candidates for local adaptations and/or genes under ongoing selection during the time span covered by our

Please cite this article in press as: Stanton et al., Paleogenomes reveal the evolutionary relationship between modern and cave lions, Cell (2026), https://doi.org/10.1016/j.cell.2026.05.007

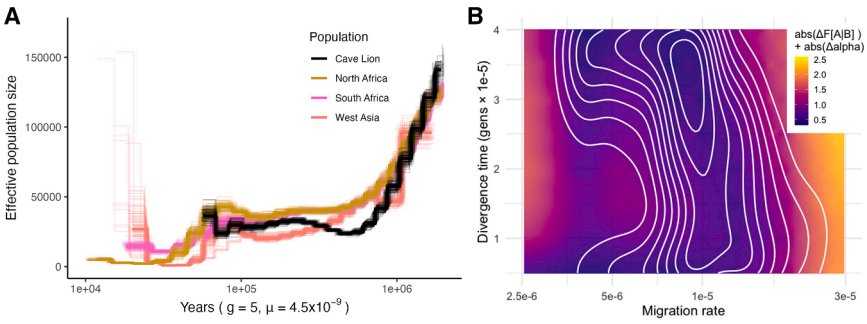

Figure 5. Demographic history of extinct and living lions

(A) PSMC analysis showing changes in effective population size for four modern lion individuals: Barbary ("Pleo_Barbary1"), Southwest Asian ("Pleo_SouthwestAsia2"), and South African ("Pleo_RSA"), of which Southwest Asian and Barbary are extinct, and one cave lion genome ("CE_Asia_20KYA"). One hundred bootstrap replicates are shown for each individual. Generation time (5 years) and mutation rate (4.5×10^{-9}) are from de Manuel et al.,[14] with years displayed on a log scale.

(B) Density plot (white lines) of plausible divergence time estimates between cave and modern lions (based on overlap between simulated and empirical F(A|B) values and migration rates). Background color corresponds to a measure of proximity of the summary statistics between the simulated and empirical data, calculated as abs(simulated F(A|B) − empirical F(A|B)) + abs(simulated F(A|B) − empirical F(A|B)).

temporal dataset (see STAR Methods, "partitioning of variation and identification of positive selection"). We then identified whether these corresponded with overrepresented biological functions, using a Gene Ontology (GO) analysis.[58,59]

Due to the low number of fixed, derived, non-synonymous mutations in cave lions, the McDonald-Kreitman test did not identify any clear signals of selection in the genomes studied. However, as this test focuses only on fixed variation across all genomes sampled, any signal of selection would not be evident if an allele was only locally fixed or became fixed during the time period covered by our samples. However, we did identify 33 mutations predicted to have a high level of disruptive protein impact that were fixed in, and unique to, the cave lion lineage (Table S3).

We also identified numerous genes with an excess of *de novo*, non-synonymous mutations in cave lions. Many of the overrepresented biological functions associated with these genes relate to biologically meaningful diversifications in morphology and physiology. In particular, several functions relating to the brain, central nervous system, vision, circulatory system development, and growth (Figure 6), which we hypothesize to be under ongoing selection. Although we note that our current sample size is not large enough to explicitly test directional selection in these genes, they provide promising candidates for future studies focusing on cave lion adaptation to the Holarctic ecosystems of the Late Pleistocene.

Conclusions

Our results demonstrate that cave and modern lions were distinct evolutionary lineages across their whole-genome and spatial distribution, with independent demographic trajectories. We show that lineage-specific mutations have led to considerable functional differentiation at numerous sites throughout the cave lion genome. We also detect an excess of non-synonymous variation in cave lion genes associated with the brain, central nervous system, vision, circulatory system development, and growth. These findings are consistent with local adaptation and/or ongoing selection in cave lions spanning our sampling period, a hypothesis that could be tested with additional specimens.

We carried out an extensive analysis of the temporal and spatial genomic structure of cave lions and detected several parallels with an extant contemporaneous carnivore, the wolf. We detected extensive population connectivity, with evidence of ancestry being replaced across the cave lion distribution, as well as with minority fractions of local deep ancestry persisting in the North American and European genomes. In North American wolves, this deep ancestry is explained by coyote[25] or red wolf[50] introgression, whereas for North American cave lions, we hypothesize that this is due to admixture with the extinct American lion.

Cave lions showed a distinct demographic history from modern lions from c. 1 mya, with a lower effective population size for cave lions throughout the majority of their history. This holds true until the most recent time estimates, when the magnitude is reversed, a notable observation for modern lion conservation, given what we know about the subsequent decline and eventual extinction of the cave lion. Despite this considerable demographic and genetic differentiation between the lion lineages, they were able to interbreed, and we detected multiple signals of modern-cave lion introgression during the Late Pleistocene. Before going extinct, cave lions appear to have interbred with modern lions in the northernmost part of the modern lion distribution. This modern lion ancestry occurs at levels of up to 3.2%–4.4% of the genome in cave lion individuals, and the level of introgression appears to be associated with glacial extent, being at highest levels during the Last Glacial Maximum. The most likely modern lion candidates for these introgression events are Southwest Asian lions, a northern population of modern lions that itself went extinct in the 20th century. We did not identify any gene-flow signals that suggested additional contact zones, for instance, the Balkans; however, additional (higher coverage) specimens from Europe would be required to fully test this hypothesis. Our observations are consistent with a situation in which the cave lion distribution expanded south during periods of increased global ice volume in the Late Pleistocene, driving an increased rate of introgression.

Limitations of the study

In this study, we investigated the evolutionary history of cave lions within the broader context of the modern lion lineage, using genomes spanning the Late Pleistocene. Although the sample size is limited, the spatial and temporal distribution of the genomes from both extinct and extant species makes this a uniquely valuable dataset. Using these data, we identified gene

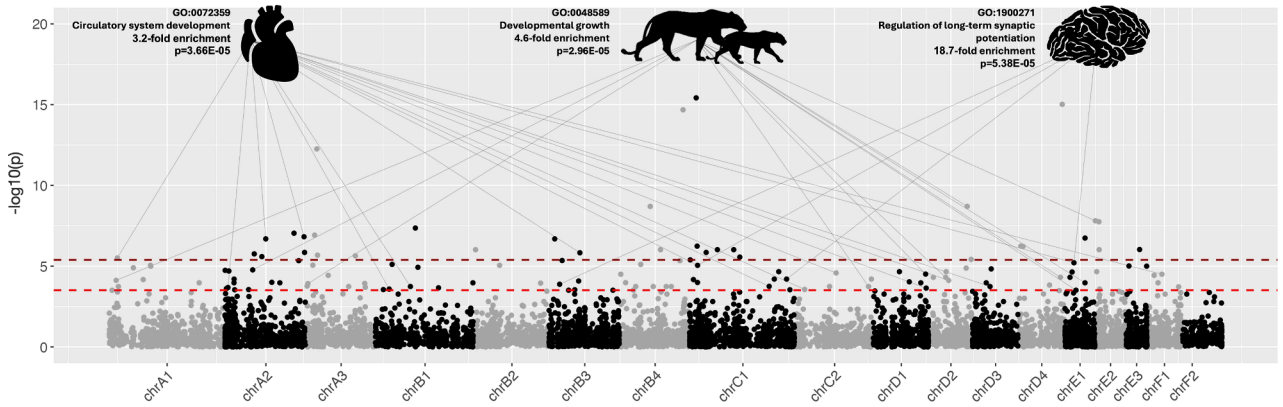

Figure 6. Candidate genes hypothesized as being under selection in the cave lion

These genes were identified as having an excess of non-synonymous mutations on the cave lion lineage, relative to synonymous mutations (with significance assessed using chi-squared tests [−log10(*p*)]). Dashed red and dark red lines show the top 1% significant and Bonferroni-corrected *p* values, respectively. A subset of biological functions that are overrepresented within the top 1% of the candidate genes (based on *p* values, see Tables S4 and S5) are identified with solid lines connected to the genes with the corresponding GO annotations.

flow between modern and cave lions and found that levels of introgression were strongly correlated with a proxy for historical global ice extent. Although this correlation was stronger than that with time alone, the difference was not statistically significant.

We also identified genes in cave lions with an excess of *de novo*, non-synonymous mutations associated with biologically meaningful changes in morphology and physiology. Although our current sample size is not sufficient to explicitly test for directional selection in these genes, they represent promising candidates for future studies on cave lion adaptation to Holarctic ecosystems during the Late Pleistocene.

RESOURCE AVAILABILITY

Lead contact

Further information and requests for resources should be directed to and will be fulfilled by the lead contact, David Stanton (stantondw@cardiff.ac.uk).

Materials availability

This study did not generate new, unique reagents.

Data and code availability

- All short-read sequencing data generated in this study have been deposited in the European Nucleotide Archive (ENA) under project accession PRJEB83684. Individual experiment accessions are available under ERX13487333–ERX13500950 and are listed in Table S2.
- All original code used to perform forward simulations has been deposited at Zenodo (DOI: https://doi.org/10.5281/zenodo.19890537) and is publicly available as of the date of publication.
- Any additional information required to reanalyze the data reported in this paper is available from the lead contact upon request.

ACKNOWLEDGMENTS

We would like to acknowledge Semyon Grigoriev, who sadly passed away during this project. Semyon was a highly valued friend and colleague who made significant contributions to Siberian paleontology. We also acknowledge Laura Bertola for comments on an earlier version of the manuscript. We kindly thank Asier Gomez, Alain Argant, Lisa Janz, Frank Zachos, Anthony Stuart, Adrian Lister, and Ian Barnes for samples and sampling support and Marc de Manuel for assistance with analyses. D.W.G.S. acknowledges support from the European Union's Horizon 2020 research and innovation programme, under the Marie Skłodowska-Curie grant agreement no. 796877, and the Cardiff Ancient Biomolecules Lab. L.D. acknowledges support from the Swedish Research Council (2021-00625) and the European Union (ERC, PrimiGenomes, 101054984). M.K. has been funded by the Vienna Science and Technology Fund (WWTF) (10.47379/VRG20001) and the "la Caixa" Foundation (ID 100010434), fellowship code LCF/BQ/PR19/11700002. We also acknowledge support from the Science for Life Laboratory, the National Genomics Infrastructure, and UPPMAX for providing assistance in massive parallel sequencing and computational infrastructure.

AUTHOR CONTRIBUTIONS

D.W.G.S. and L.D. conceived and led the study. D.W.G.S., M.S.-V., and E.E. processed the samples in the lab. D.W.G.S. analyzed the data, with guidance from A.B., P.D.H., A.C., M.K., P.S., and L.F. R.B., M.-H.S.S., T. M.-B., N.Y., M.T.P.G., D.N., V.P., A.P., M.S.-V., S.A., S.F., E.E., and L.D. contributed important resources. D.W.G.S. and L.D. wrote the manuscript, with input from all co-authors.

DECLARATION OF INTERESTS

The authors declare no competing interests.

STAR★METHODS

Detailed methods are provided in the online version of this paper and include the following:

- KEY RESOURCES TABLE
- EXPERIMENTAL MODEL AND STUDY PARTICIPANT DETAILS
- METHOD DETAILS
  - Sample collection and dating
  - Molecular lab work and sequencing
- QUANTIFICATION AND STATISTICAL ANALYSIS
  - Bioinformatic pre-processing
  - Variant calling and ascertainment panel
  - Pseudohaploid dataset generation
  - Population and phylogenetic analysis
  - Population Genetic Structure And Exploratory Gene Flow Analysis
  - Shared ancestry and admixture proportion calculations
  - Cave lion genetic structure
  - f4(Out, Cave-X[Eastern Eurasia]; Cave[N.America], Cave[Europe])

- f4(Out, Cave[Siberia,Age-X]; Cave[Region=N.America/Europe/-C.E.Asia], Cave[Recent Siberia])
- Timing ancestry homogenisation in cave lions
- Admixture graphs
- Demographic inference
- Lion divergence times
- Partitioning of variation and identification of positive selection

SUPPLEMENTAL INFORMATION

Supplemental information can be found online at https://doi.org/10.1016/j.cell.2026.05.007.

Received: December 17, 2024
Revised: November 7, 2025
Accepted: May 6, 2026

REFERENCES

1. Barnett, R., Shapiro, B., Barnes, I., Ho, S.Y.W., Burger, J., Yamaguchi, N., Higham, T.F.G., Wheeler, H.T., Rosendahl, W., Sher, A.V., et al. (2009). Phylogeography of lions (Panthera leo ssp.) reveals three distinct taxa and a late Pleistocene reduction in genetic diversity. Mol. Ecol. *18*, 1668–1677. https://doi.org/10.1111/j.1365-294X.2009.04134.x.
2. Kurtén, B. (2017). Pleistocene Mammals of Europe (Routledge). https://doi.org/10.4324/9781315126470.
3. Yamaguchi, N., Cooper, A., Werdelin, L., and Macdonald, D.W. (2004). Evolution of the mane and group-living in the lion (Panthera leo): a review. J. Zool. *263*, 329–342. https://doi.org/10.1017/S0952836904005242.
4. Stuart, A.J., and Lister, A.M. (2007). Patterns of Late Quaternary megafaunal extinctions in Europe and northern Asia. Cour. Forschungsinst. Senckenb. *259*, 287–297.
5. Reynaud Savioz, N., and Elsuede, H. (2017). Les carnivores pléistocènes des genres Canis et Panthera de Hummal et Nadaouiyeh Aïn Askar (El Kowm, Syrie). ERAUL *148*, 109–119.
6. Argant, A., and Brugal, J.-P. (2017). The cave lion Panthera (Leo) spelaea and its evolution: Panthera spelaea intermedia nov. subspecies. Acta Zool. Cracoviensia *60*, 58–103. https://doi.org/10.3409/azc.60_2.59.
7. Lewis, M., Pacher, M., and Turner, A. (2010). The larger Carnivora of the West Runton Freshwater Bed. Quat. Int. *228*, 116–135. https://doi.org/10.1016/j.quaint.2010.06.022.
8. Sala, B. (1990). Panthera leo fossilis (v. Reich., 1906) (Felidae) de Isernia la Pineta (Pléistocène moyen inférieur d'Italie. Geobios *23*, 189–194. https://doi.org/10.1016/S0016-6995(06)80051-3.
9. Kurtén, B., and Anderson, E. (1980). Pleistocene Mammals of North America (Columbia University Press).
10. Boeskorov, G.G., Plotnikov, V.V., Protopopov, A.V., Baryshnikov, G.F., Fosse, P., Dalén, L., Stanton, D.W.G., Pavlov, I.S., Suzuki, N., and Tikhonov, A.N. (2021). The Preliminary Analysis of Cave Lion Cubs Panthera spelaea (Goldfuss, 1810) from the Permafrost of Siberia. Quaternary *4*, 24. https://doi.org/10.3390/quat4030024.
11. Stuart, A.J., and Lister, A.M. (2011). Extinction chronology of the cave lion Panthera spelaea. Quat. Sci. Rev. *30*, 2329–2340. https://doi.org/10.1016/j.quascirev.2010.04.023.
12. Bocherens, H. (2015). Isotopic tracking of large carnivore palaeoecology in the mammoth steppe. Quat. Sci. Rev. *117*, 42–71. https://doi.org/10.1016/j.quascirev.2015.03.018.
13. Packer, C., and Clottes, J. (2000). When lions ruled France. Nat. Hist. *109*, 52–57.
14. de Manuel, M., Barnett, R., Sandoval-Velasco, M., Yamaguchi, N., Garrett Vieira, F., Zepeda Mendoza, M.L., Liu, S., Martin, M.D., Sinding, M.-H.S., Mak, S.S.T., et al. (2020). The evolutionary history of extinct and living lions. Proc. Natl. Acad. Sci. USA *117*, 10927–10934. https://doi.org/10.1073/pnas.1919423117.
15. Hoffman, J.I., Vendrami, D.L.J., Hench, K., Chen, R.S., Stoffel, M.A., Kardos, M., Amos, W., Kalinowski, J., Rickert, D., Köhrer, K., et al. (2024). Genomic and fitness consequences of a near-extinction event in the northern elephant seal. Nat. Ecol. Evol. *8*, 2309–2324. https://doi.org/10.1038/s41559-024-02533-2.
16. Barnett, R., Mendoza, M.L.Z., Soares, A.E.R., Ho, S.Y.W., Zazula, G., Yamaguchi, N., Shapiro, B., Kirillova, I.V., Larson, G., and Gilbert, M.T.P. (2016). Mitogenomics of the Extinct Cave Lion, Panthera spelaea (Goldfuss, 1810), Resolve its Position within the Panthera Cats. Open Quat. *2*, 4. https://doi.org/10.5334/oq.24.
17. Stanton, D.W.G., Alberti, F., Plotnikov, V., Androsov, S., Grigoriev, S., Fedorov, S., Kosintsev, P., Nagel, D., Vartanyan, S., Barnes, I., et al. (2020). Early Pleistocene origin and extensive intra-species diversity of the extinct cave lion. Sci. Rep. *10*, 12621. https://doi.org/10.1038/s41598-020-69474-1.
18. Figueiró, H.V., Li, G., Trindade, F.J., Assis, J., Pais, F., Fernandes, G., Santos, S.H.D., Hughes, G.M., Komissarov, A., Antunes, A., et al. (2017). Genome-wide signatures of complex introgression and adaptive evolution in the big cats. Sci. Adv. *3*, e1700299. https://doi.org/10.1126/sciadv.1700299.
19. Santos, S.H.D., Figueiró, H.V., Flouri, T., Ramalho, E., Cullen, L., Jr., Yang, Z., Murphy, W.J., and Eizirik, E. (2025). Massive inter-species introgression overwhelms phylogenomic relationships among jaguar, lion, and leopard. Syst. Biol. *74*, 583–599.
20. Sabol, M., Tomašových, A., and Gullár, J. (2022). Geographic and temporal variability in Pleistocene lion-like felids: Implications for their evolution and taxonomy. Palaeontol. Electron. *25*, a26. https://doi.org/10.26879/1175.
21. Marciszak, A., Ivanoff, D.V., Semenov, Y.A., Talamo, S., Ridush, B., Stupak, A., Yanish, Y., and Kovalchuk, O. (2023). The Quaternary lions of Ukraine and a trend of decreasing size in Panthera spelaea. J. Mammal. Evol. *30*, 109–135. https://doi.org/10.1007/s10914-022-09635-3.
22. Sabol, M., and Puzachenko, A.Y. (2024). Distribution of cave lions (Panthera spelaea ssp.) in mountain areas. Earth Hist. Biodivers. *1*, 100009. https://doi.org/10.1016/j.hisbio.2024.100009.
23. Hemmer, H. (1974). Untersuchungen zur Stammesgeschichte der Pantherkatzen (Pantherinae) - Teil III - Zur Artgeschichte des Löwen Panthera (Panthera) leo (Linnaeus 1758). Veröff. Zool. Staatssammlung München *17*, 167–280.
24. Vershinina, A.O., Heintzman, P.D., Froese, D.G., Zazula, G., Cassatt-Johnstone, M., Dalén, L., Der Sarkissian, C., Dunn, S.G., Ermini, L., Gamba, C., et al. (2021). Ancient horse genomes reveal the timing and extent of dispersals across the Bering Land Bridge. Mol. Ecol. *30*, 6144–6161. https://doi.org/10.1111/mec.15977.
25. Bergström, A., Stanton, D.W.G., Taron, U.H., Frantz, L., Sinding, M.-H.S., Ersmark, E., Pfrengle, S., Cassatt-Johnstone, M., Lebrasseur, O., Girdland-Flink, L., et al. (2022). Grey wolf genomic history reveals a dual ancestry of dogs. Nature *607*, 313–320. https://doi.org/10.1038/s41586-022-04824-9.
26. Hu, A., Meehl, G.A., Otto-Bliesner, B.L., Waelbroeck, C., Han, W., Loutre, M.-F., Lambeck, K., Mitrovica, J.X., and Rosenbloom, N. (2010). Influence of Bering Strait flow and North Atlantic circulation on glacial sea-level changes. Nat. Geosci. *3*, 118–121. https://doi.org/10.1038/ngeo729.
27. Barnosky, A.D., Koch, P.L., Feranec, R.S., Wing, S.L., and Shabel, A.B. (2004). Assessing the causes of late Pleistocene extinctions on the continents. Science *306*, 70–75. https://doi.org/10.1126/science.1101476.
28. Malhi, Y., Doughty, C.E., Galetti, M., Smith, F.A., Svenning, J.-C., and Terborgh, J.W. (2016). Megafauna and ecosystem function from the Pleistocene to the Anthropocene. Proc. Natl. Acad. Sci. USA *113*, 838–846. https://doi.org/10.1073/pnas.1502540113.

29. Barnett, R., Yamaguchi, N., Shapiro, B., and Nijman, V. (2007). Using ancient DNA techniques to identify the origin of unprovenanced museum specimens, as illustrated by the identification of a 19th century lion from Amsterdam. Contrib. Zool. *76*, 87–94. https://doi.org/10.1163/18759866-07602002.

30. Schnitzler, A.E. (2011). Past and present distribution of the North African–Asian lion subgroup: a review. Mamm. Rev. *41*, 220–243. https://doi.org/10.1111/j.1365-2907.2010.00181.x.

31. Laundré, J.W., and Hernández, L. (2010). The landscape of fear: ecological implications of being afraid. Open Ecol. J. *3*, 1–7.

32. Kitchener, A.C., and Dugmore, A.J. (2000). Biogeographical change in the tiger, Panthera tigris. Anim. Conserv. *3*, 113–124. https://doi.org/10.1111/j.1469-1795.2000.tb00236.x.

33. Hemmer, H., Kahlke, R.-D., and Vekua, A.K. (2001). The Jaguar - Panthera onca gombaszoegensis (Kretzoi, 1938) (Carnivora: Felidae) in the late lower pleistocene of Akhalkalaki (south Georgia; Transcaucasia) and its evolutionary and ecological significance. Geobios *34*, 475–486. https://doi.org/10.1016/s0016-6995(01)80011-5.

34. Estes, J.A., Terborgh, J., Brashares, J.S., Power, M.E., Berger, J., Bond, W.J., Carpenter, S.R., Essington, T.E., Holt, R.D., Jackson, J.B.C., et al. (2011). Trophic downgrading of planet Earth. Science *333*, 301–306. https://doi.org/10.1126/science.1205106.

35. Burger, J., Rosendahl, W., Loreille, O., Hemmer, H., Eriksson, T., Götherström, A., Hiller, J., Collins, M.J., Wess, T., and Alt, K.W. (2004). Molecular phylogeny of the extinct cave lion Panthera leo spelaea. Mol. Phylogenet. Evol. *30*, 841–849. https://doi.org/10.1016/j.ympev.2003.07.020.

36. Li, G., Figueiró, H.V., Eizirik, E., and Murphy, W.J. (2019). Recombination-aware phylogenomics reveals the structured genomic landscape of hybridizing cat species. Mol. Biol. Evol. *36*, 2111–2126. https://doi.org/10.1093/molbev/msz139.

37. Li, G., Davis, B.W., Eizirik, E., and Murphy, W.J. (2016). Phylogenomic evidence for ancient hybridization in the genomes of living cats (Felidae). Genome Res. *26*, 1–11. https://doi.org/10.1101/gr.186668.114.

38. Kim, S., Cho, Y.S., Kim, H.-M., Chung, O., Kim, H., Jho, S., Seomun, H., Kim, J., Bang, W.Y., Kim, C., et al. (2016). Comparison of carnivore, omnivore, and herbivore mammalian genomes with a new leopard assembly. Genome Biol. *17*, 211. https://doi.org/10.1186/s13059-016-1071-4.

39. Huntley, B., Allen, J.R.M., Forrest, M., Hickler, T., Ohlemüller, R., Singarayer, J.S., and Valdes, P.J. (2023). Global biome patterns of the Middle and Late Pleistocene. J. Biogeogr. *50*, 1352–1372. https://doi.org/10.1111/jbi.14619.

40. Bouckaert, R.R. (2010). DensiTree: making sense of sets of phylogenetic trees. Bioinformatics *26*, 1372–1373. https://doi.org/10.1093/bioinformatics/btq110.

41. Stamatakis, A. (2014). RAxML version 8: a tool for phylogenetic analysis and post-analysis of large phylogenies. Bioinformatics *30*, 1312–1313. https://doi.org/10.1093/bioinformatics/btu033.

42. Nicholson, S., Bauer, H., Strampelli, P., Sogbohossou, E., Ikanda, D., Tumenta, P.F., Venktraman, M., Chapron, G., and Loveridge, A. (2023). *Panthera leo* (amended version of 2023 assessment) (The IUCN Red List of Threatened Species). https://www.iucnredlist.org/species/15951/259030422.

43. Ersmark, E., Orlando, L., Sandoval-Castellanos, E., Barnes, I., Barnett, R., Stuart, A., Lister, A., and Dalén, L. (2015). Population Demography and Genetic Diversity in the Pleistocene Cave Lion. OPEN QUAT *1*, 4. https://doi.org/10.5334/oq.aa.

44. Thapar, V., and Ansari, Y. (2013). Exotic Aliens: The Lion & the Cheetah in India (Aleph Book Company).

45. O'Brien, S.J., Joslin, P., Smith, G.L., III, Wolfe, R., Schaffer, N., Heath, E., Ott-Joslin, J., Rawal, P.P., Bhattacharjee, K.K., and Martenson, J.S. (1987). Evidence for African origins of founders of the asiatic lion species survival plan. Zoo Biol. *6*, 99–116. https://doi.org/10.1002/zoo.1430060202.

46. Driscoll, C.A., Menotti-Raymond, M., Nelson, G., Goldstein, D., and O'Brien, S.J. (2002). Genomic microsatellites as evolutionary chronometers: a test in wild cats. Genome Res. *12*, 414–423. https://doi.org/10.1101/gr.185702.

47. Tseng, Z.J., Wang, X., Slater, G.J., Takeuchi, G.T., Li, Q., Liu, J., and Xie, G. (2014). Himalayan fossils of the oldest known pantherine establish ancient origin of big cats. Proc. R. Soc. B. *281*, 20132686. https://doi.org/10.1098/rspb.2013.2686.

48. Johnson, W.E., Eizirik, E., Pecon-Slattery, J., Murphy, W.J., Antunes, A., Teeling, E., and O'Brien, S.J. (2006). The late Miocene radiation of modern Felidae: a genetic assessment. Science *311*, 73–77. https://doi.org/10.1126/science.1122277.

49. Yuan, J., Wang, G., Zhao, L., Kitchener, A.C., Sun, T., Chen, W., Huang, C., Wang, C., Xu, X., Wang, J., et al. (2023). How genomic insights into the evolutionary history of clouded leopards inform their conservation. Sci. Adv. *9*, eadh9143. https://doi.org/10.1126/sciadv.adh9143.

50. Sacks, B.N., Mitchell, K.J., Quinn, C.B., Hennelly, L.M., Sinding, M.-H.S., Statham, M.J., Preckler-Quisquater, S., Fain, S.R., Kistler, L., Vanderzwan, S.L., et al. (2021). Pleistocene origins, western ghost lineages, and the emerging phylogeographic history of the red wolf and coyote. Mol. Ecol. *30*, 4292–4304. https://doi.org/10.1111/mec.16048.

51. Salis, A.T., Bray, S.C.E., Lee, M.S.Y., Heiniger, H., Barnett, R., Burns, J.A., Doronichev, V., Fedje, D., Golovanova, L., Harington, C.R., et al. (2022). Lions and brown bears colonized North America in multiple synchronous waves of dispersal across the Bering Land Bridge. Mol. Ecol. *31*, 6407–6421. https://doi.org/10.1111/mec.16267.

52. Lisiecki, L.E., and Stern, J.V. (2016). Regional and global benthic $\delta^{18}O$ stacks for the last glacial cycle. Paleoceanogr. Paleoclimatol. *31*, 1368–1394. https://doi.org/10.1002/2016PA003002.

53. Kitchener, A.C., Breitenmoser-Würsten, C., Eizirik, E., Gentry, A., Werdelin, L., Wilting, A., Yamaguchi, N., Abramov, A.V., Christiansen, P., Driscoll, C., et al. (2017). A revised taxonomy of the Felidae: The final report of the Cat Classification Task Force of the IUCN Cat Specialist Group. Cat News *11*, 80.

54. Daróczi-Szabó, M., Kovács, Z.E., Raczky, P., and Bartosiewicz, L. (2020). Pending danger: Recent Copper Age lion (Panthera leo L., 1758) finds from Hungary. Int. J. Osteoarchaeol. *30*, 469–481. https://doi.org/10.1002/oa.2875.

55. McDonald, J.H., and Kreitman, M. (1991). Adaptive protein evolution at the Adh locus in Drosophila. Nature *351*, 652–654. https://doi.org/10.1038/351652a0.

56. Cingolani, P., Platts, A., Wang, L.L., Coon, M., Nguyen, T., Wang, L., Land, S.J., Lu, X., and Ruden, D.M. (2012). A program for annotating and predicting the effects of single nucleotide polymorphisms, SnpEff: SNPs in the genome of Drosophila melanogaster strain w^{1118}; iso-2; iso-3. Fly *6*, 80–92. https://doi.org/10.4161/fly.19695.

57. Cingolani, P. (2026). Input & output files. GitHub. https://pcingola.github.io/SnpEff/se_inputoutput/.

58. Aleksander, S.A., Balhoff, J., Carbon, S., Cherry, J.M., Drabkin, H.J., Ebert, D., Feuermann, M., Gaudet, P., Harris, N.L., Hill, D.P., et al. (2023). The Gene Ontology knowledgebase in 2023. Genetics *224*, iyad031. https://doi.org/10.1093/genetics/iyad031.

59. Ashburner, M., Ball, C.A., Blake, J.A., Botstein, D., Butler, H., Cherry, J.M., Davis, A.P., Dolinski, K., Dwight, S.S., Eppig, J.T., et al. (2000). Gene ontology: tool for the unification of biology. Nat. Genet. *25*, 25–29. https://doi.org/10.1038/75556.

60. St. John, J. (2016). SeqPrep GitHub. https://github.com/jstjohn/SeqPrep.

61. Li, H., and Durbin, R. (2010). Fast and accurate long-read alignment with Burrows–Wheeler transform. Bioinformatics *26*, 589–595. https://doi.org/10.1093/bioinformatics/btp698.

62. Li, H. (2011). vcfutils.pl at master lh3/samtools GitHub. https://github.com/lh3/samtools/blob/master/bcftools/vcfutils.pl.

63. Li, H. (2011). A statistical framework for SNP calling, mutation discovery, association mapping and population genetical parameter estimation from sequencing data. Bioinformatics *27*, 2987–2993. https://doi.org/10.1093/bioinformatics/btr509.

64. Purcell, S., Neale, B., Todd-Brown, K., Thomas, L., Ferreira, M.A.R., Bender, D., Maller, J., Sklar, P., de Bakker, P.I.W., Daly, M.J., et al. (2007). PLINK: a tool set for whole-genome association and population-based linkage analyses. Am. J. Hum. Genet. *81*, 559–575. https://doi.org/10.1086/519795.

65. McKenna, A., Hanna, M., Banks, E., Sivachenko, A., Cibulskis, K., Kernytsky, A., Garimella, K., Altshuler, D., Gabriel, S., Daly, M., et al. (2010). The Genome Analysis Toolkit: a MapReduce framework for analyzing next-generation DNA sequencing data. Genome Res. *20*, 1297–1303. https://doi.org/10.1101/gr.107524.110.

66. Baumdicker, F., Bisschop, G., Goldstein, D., Gower, G., Ragsdale, A.P., Tsambos, G., Zhu, S., Eldon, B., Ellerman, E.C., Galloway, J.G., et al. (2022). Efficient ancestry and mutation simulation with msprime 1.0. Genetics *220*, iyab229. https://doi.org/10.1093/genetics/iyab229.

67. Skoglund, P. (2020). samremovedup.py at master pontussk/samremovedup GitHub. https://github.com/pontussk/samremovedup/blob/master/samremovedup.py.

68. Quinlan, A.R., and Hall, I.M. (2010). BEDTools: a flexible suite of utilities for comparing genomic features. Bioinformatics *26*, 841–842. https://doi.org/10.1093/bioinformatics/btq033.

69. Li, H. (2025). htsbox: My experimental tools on top of htslib GitHub. https://github.com/lh3/htsbox.

70. Palkopoulou, E., Mallick, S., Skoglund, P., Enk, J., Rohland, N., Li, H., Omrak, A., Vartanyan, S., Poinar, H., Götherström, A., et al. (2015). Complete genomes reveal signatures of demographic and genetic declines in the woolly mammoth. Curr. Biol. *25*, 1395–1400. https://doi.org/10.1016/j.cub.2015.04.007.

71. Flynn, J.M., Hubley, R., Goubert, C., Rosen, J., Clark, A.G., Feschotte, C., and Smit, A.F. (2020). RepeatModeler2 for automated genomic discovery of transposable element families. Proc. Natl. Acad. Sci. USA *117*, 9451–9457. https://doi.org/10.1073/pnas.1921046117.

72. Günther, T., and Nettelblad, C. (2019). The presence and impact of reference bias on population genomic studies of prehistoric human populations. PLoS Genet. *15*, e1008302. https://doi.org/10.1371/journal.pgen.1008302.

73. Skoglund, P., Mallick, S., Bortolini, M.C., Chennagiri, N., Hünemeier, T., Petzl-Erler, M.L., Salzano, F.M., Patterson, N., and Reich, D. (2015). Genetic evidence for two founding populations of the Americas. Nature *525*, 104–108. https://doi.org/10.1038/nature14895.

74. Skoglund, P. (2018). popstats: Population genetic summary statistics GitHub. https://github.com/pontussk/popstats.

75. RepeatMasker (2025). http://www.repeatmasker.org.

76. Renaud, G. (2022). mappability_snpable GitHub. https://github.com/grenaud/mappability_snpable.

77. Pickrell, J.K., and Pritchard, J.K. (2012). Inference of population splits and mixtures from genome-wide allele frequency data. PLoS Genet. *8*, e1002967. https://doi.org/10.1371/journal.pgen.1002967.

78. Patterson, N., Moorjani, P., Luo, Y., Mallick, S., Rohland, N., Zhan, Y., Genschoreck, T., Webster, T., and Reich, D. (2012). Ancient admixture in human history. Genetics *192*, 1065–1093. https://doi.org/10.1534/genetics.112.145037.

79. Maier, R. (2022) Admixture graphs. https://uqrmaie1.github.io/admixtools/articles/graphs.html?q=out%20of%20sample.

80. Armstrong, E.E., Taylor, R.W., Miller, D.E., Kaelin, C.B., Barsh, G.S., Hadly, E.A., and Petrov, D. (2020). Long live the king: chromosome-level assembly of the lion (Panthera leo) using linked-read, Hi-C, and long-read data. BMC Biol. *18*, 3. https://doi.org/10.1186/s12915-019-0734-5.

81. Li, H., and Durbin, R. (2011). Inference of human population history from individual whole-genome sequences. Nature *475*, 493–496. https://doi.org/10.1038/nature10231.

82. Green, R.E., Krause, J., Briggs, A.W., Maricic, T., Stenzel, U., Kircher, M., Patterson, N., Li, H., Zhai, W., Fritz, M.H.-Y., et al. (2010). A draft sequence of the Neandertal genome. Science *328*, 710–722. https://doi.org/10.1126/science.1188021.

83. Fitak, R.R. (2021). OptM: estimating the optimal number of migration edges on population trees using Treemix. Biol. Methods Protoc. *6*, bpab017. https://doi.org/10.1093/biomethods/bpab017.

Please cite this article in press as: Stanton et al., Paleogenomes reveal the evolutionary relationship between modern and cave lions, Cell (2026), https://doi.org/10.1016/j.cell.2026.05.007

CellPress
OPEN ACCESS

STAR★METHODS

KEY RESOURCES TABLE

REAGENT or RESOURCE	SOURCE	IDENTIFIER
Biological samples		
Cave Lion	Austria_17KYA	Ersmark et al.[43]
Cave Lion	Yukon_33KYA	Barnett et al.[16]
Cave Lion	Siberia_44KYA	Present Study
Cave Lion	Siberia_30KYA	Stanton et al.[17]
Cave Lion	SiberiaA_33KYA	Stanton et al.[17]
Cave Lion	NSI_52KYA	Ersmark et al.[43]
Cave Lion	Siberia_47KYA	Stanton et al.[17]
Cave Lion	Siberia_22KYA	Ersmark et al.[43]
Cave Lion	Siberia_148KYA	Ersmark et al.[43]
Cave Lion	Siberia_64KYA	Stanton et al.[17]
Cave Lion	SiberiaB_33KYA	de Manuel et al.[14]
Cave Lion	CE_Asia_20KYA	Ersmark et al.[43]
Modern lion	Pleo_SouthwestAsia1	de Manuel et al.[14]
Modern lion	Pleo_Barbary2	de Manuel et al.[14]
Modern lion	Pleo_Barbary3	de Manuel et al.[14]
Modern lion	Pleo_Cape2	de Manuel et al.[14]
Modern lion	Pleo_SouthwestAsia3	Present study
Modern lion	Pleo_Gabon	de Manuel et al.[14]
Modern lion	Pleo_Senegal2	de Manuel et al.[14]
Modern lion	Pleo_India1	de Manuel et al.[14]
Modern lion	Pleo_Tanzania2	de Manuel et al.[14]
Modern lion	Pleo_Tanzania1	de Manuel et al.[14]
Modern lion	Pleo_India2	de Manuel et al.[14]
Modern lion	Pleo_Botswana1	de Manuel et al.[14]
Modern lion	Pleo_Botswana2	de Manuel et al.[14]
Modern lion	Pleo_Senegal1	de Manuel et al.[14]
Modern lion	Pleo_Cape1	de Manuel et al.[14]
Modern lion	Pleo_Sudan	de Manuel et al.[14]
Modern lion	Pleo_SouthwestAsia2	de Manuel et al.[14]
Modern lion	Pleo_RSA	de Manuel et al.[14]
Modern lion	Pleo_Barbary1	de Manuel et al.[14]
Modern lion	Pleo_Captive2	de Manuel et al.[14]
Modern lion	Pleo_Captive1	de Manuel et al.[14]
Felid outgroup	Siberian	Kim et al.[38]
Felid outgroup	SnowLeopard	Kim et al.[38]
Felid outgroup	Bengal	Kim et al.[38]
Felid outgroup	CloudedLeopard	de Manuel et al.[14]
Felid outgroup	Pantheraonca	Figueiró et al.[18]
Felid outgroup	Pantherapardus	Kim et al.[38]
Chemicals peptides and recombinant proteins		
USER enzyme	New England Biolabs	NEB #M5508
AccuPrime reaction mix	Life Technologies	Cat #12344040
AccuPrime Pfx DNA polymerase	Life Technologies	Cat #12344024

(*Continued on next page*)

Please cite this article in press as: Stanton et al., Paleogenomes reveal the evolutionary relationship between modern and cave lions, Cell (2026), https://doi.org/10.1016/j.cell.2026.05.007

Continued

REAGENT or RESOURCE	SOURCE	IDENTIFIER
EDTA	ThermoFisher Scientific	Cat #15575020
UREA	VWR	Cat #443874G
Proteinase K	VWR	Cat #1.24568.0100
Tango Buffer (10X)	ThermoFisher Scientific	Cat #BY5
ATP (100mM)	ThermoFisher Scientific	Cat #R0441
T4 Polynucleotide Kinase (10U/ul)	ThermoFisher Scientific	Cat #EK0032
T4 DNA Polymerase (5U/ul)	ThermoFisher Scientific	Cat #EP0062
T4 DNA Ligase (5U/ul)	ThermoFisher Scientific	Cat #EL0011
Bst Polymerase, LF (8U/ul)	New England Biolabs	Cat #M0275S
Agencourt AMPure XP beads	Beckman Coulter	Cat #10136224
Critical commercial assays		
MinElute PCR purification kit	QIAGEN	Cat #28115
QiaQuick PCR purification kit	QIAGEN	Cat #28106
Agilent High Sensitivity kit	Agilent	Cat #5067-4626
Deposited data		
Raw sequencing data	This study	ENA: PRJEB83684
Software and algorithms		
SeqPrep v1.137	St. John[60]	https://github.com/jstjohn/SeqPrep
BWA v0.7.17	Li and Durbin[61]	https://bio-bwa.sourceforge.net/
SAMtools v1.9	Li[62]	http://www.htslib.org/
bcftools v1.8	Li[63]	http://www.htslib.org/
PLINK v1.9	Purcell et al.[64]	https://www.cog-genomics.org/plink2
SNPeff v5.0	Cingolani et al.[56] and Cingolani[57]	http://snpeff.sourceforge.net/index.html
GATK v3.7	McKenna et al.[65]	https://gatk.broadinstitute.org/hc/en-us
Msprime v1.2.0	Baumdicker et al.[66]	https://tskit.dev/msprime/docs/stable/intro.html
Samremovedup	Skoglund[67]	https://github.com/NBISweden/GenErode/blob/main/workflow/scripts/samremovedup.py
BEDtools v2.27.1	Quinlan and Hall[68]	https://bedtools.readthedocs.io/en/latest/
Htsbox	Li[69]	https://github.com/lh3/htsbox

EXPERIMENTAL MODEL AND STUDY PARTICIPANT DETAILS

This study analysed subfossil remains of *Panthera spelaea* (cave lion), radiocarbon-dated to c. >16,803 years before present (listed in the key resources table, and Table S1). The material does not constitute living experimental animals, human participants, or extant biological models.

METHOD DETAILS

Sample collection and dating

We generated whole genome sequences from 10 cave lion samples, following an initial screening of 52 specimens. We ^{14}C dated the one specimen that had not previously been dated, and for the samples that were beyond the ^{14}C limit, we used the mitochondrial tip dates estimated in Stanton et al. (n=4; Table S1).[17] For these, the younger "tip-date only" estimates were used as these dates were more in line with the most up-to-date estimate for the modern-cave lion divergence.[14] We also sequenced the genome of a lion specimen from Southwest Asia, following the methods described in de Manuel et al.[14] and added all these newly sequenced genomes to 20 already sequenced modern lion genomes from de Manuel et al.[14] and six outgroup felid species (see Table S1). Basic library information for the newly generated genomes is given in Table S2.

Molecular lab work and sequencing

For the ten new cave lion genomes included in the present study (Table S1), DNA was extracted and sequencing libraries prepared following the methodology of Stanton et al.[17] These libraries were used as stock for between 9-13 indexing PCR amplifications per

Please cite this article in press as: Stanton et al., Paleogenomes reveal the evolutionary relationship between modern and cave lions, Cell (2026), https://doi.org/10.1016/j.cell.2026.05.007

sample using double-unique p5–p7 indexed primers and then pooled. Pools were purified and size selected using Agencourt AMPure XP beads (Beckman Coulter, Brea, CA, USA) to remove long and short fragments and quantified on a Bioanalyzer 2100 (Agilent, Santa Clara, CA, USA). The pools were sequenced across four Illumina NovaSeq6000 S4 (150 bp paired-end [PE] setup) lanes (two full lanes and two quarter lanes) at the SciLifeLab sequencing facility in Stockholm.

QUANTIFICATION AND STATISTICAL ANALYSIS

Bioinformatic pre-processing

Sequencing reads were trimmed and overlapping reads merged using SeqPrep v1.137,[60] with default settings but with a minor modification in the source code, allowing us to choose the best quality scores of bases in the merged region instead of aggregating the scores following Palkopoulou et al.[70] We hard masked repeat regions in the cat genome (Felis_catus_9.0, GCA_000181335.3) using RepeatModeller v1.0.11.[71] Merged reads ≥35 bp were then mapped to this masked genome using BWA-ALN v0.7.13,[61] using deactivated seeding (−l 16,500), more substitutions (−n 0.01), and allowing up to two gaps (−o 2). Duplicates were removed (separately for each PCR reaction) using a custom perl script that removes reads with identical start and end positions, keeping the first observed such read.[67] Indels were realigned using GATK v3.7.[65]

Variant calling and ascertainment panel

When mapping to a haploid genome, DNA fragments carrying the reference allele are more likely to map successfully. The short read lengths in ancient DNA studies increase the proportion of multiple matching sites in the genome, potentially exacerbating the impact of this bias on downstream analysis.[72] In order to investigate the extent to which reference bias was affecting our genotype calls, we carried out f4 tests using popstats,[73,74] using the setup f4(outgroup [leopard], Lion X, Reference, cat). In this formulation, reference bias would appear as consistent attraction between Lion X and the reference, in the form of significant negative values. This test was initially carried out on the full (transversions only) set of SNPs (n = 8,166,803 SNPs) that was ascertained across all lion samples (both modern and cave lion). This dataset showed clear evidence of reference bias, with all samples showing significant negative f4 values (Figure S1A). In addition, sample age appeared to be associated with the amount of reference bias, with all historic and ancient samples showing lower f4 values than the modern ones. In order to account for this reference bias, we instead ascertained SNPs in a set of eight high coverage individuals (>18X; Bengal tiger, clouded leopard, jaguar, leopard, Siberian tiger, snow leopard, modern lion and cave lion) and used this panel to ascertain variants across all individuals (Supplementary Text and Figures, "SNP Ascertainment", Figure S1). For these high coverage individuals, we called variants using bcftools v1.8,[63] filtering out base and mapping qualities lower than 30, sites with depths <1/3 or >2X the genome-wide average, removed sites within 5 bp of an indel, sites within repeat regions (using RepeatMasker v 4.1.2[71,75]), sites from genomic regions with poor mappability properties,[76] and sites where one of the alleles was observed in <20% of the reads. The same test as above for reference bias was again carried out, leading to a substantial shift towards zero for all individuals (Figure S1B), with most tests having non-significant f4-values and overlapping standard error bars between all samples and sample types. Following these filtering steps, the high-coverage SNP panel contained 1,100,134 SNPs, and was therefore used for all SNP-based analyses.

Pseudohaploid dataset generation

The above ascertainment panel was used to identify pseudohaploid calls across all individuals. First, a pseudohaploid genome was created, by randomly selecting reads from the above bam files using htsbox[69] following duplicate removal, indel realignment, and <35 bp read-length filtering. These pseudohaploid genomes were then converted and combined into a vcf file, keeping only sites from the above ascertainment panel. Transitions were then filtered out from the final, combined vcf file.

Population and phylogenetic analysis

We used TreeMix[77] and DensiTree[40] in order to investigate relationships within and between lion populations. We built phylogenies using RAxML[41] on 2, 1 and 0.5 MB, pseudohaploidized non-overlapping sliding windows for all genomes with >1X coverage, with a GTR+G substitution model, and then jointly visualised the phylogenies using DensiTree (Figure 1B). To investigate the effect of sliding window size, DNA damage, and the placement of the European cave lion genome, we repeated this analysis with window sizes of 2 Mb, 1 Mb and 500 Kb, this time including the European individual ("Austria_17KYA"), and both including and excluding transitions. We then counted the number of tree topologies for each of these situations whereby modern and cave lions were reciprocally monophyletic, and instances where the European genome was basal to the other cave lion genomes. For TreeMix, we excluded individuals with <1X mean genome coverage, and removed sites with missing data, leading to a dataset of 25 individuals (15 modern lions, 9 cave lions and 1 outgroup) and 393,645 sites, and ran the analysis with 0-5 admixture edges (Figures S2D–S2F).

Population Genetic Structure And Exploratory Gene Flow Analysis

In order to describe genetic structure and identify potential instances of gene flow between lion populations and outgroups, we used an exploratory admixture graph analysis in AdmixTools 2.0.0, on a subset of cave lions, modern lions and outgroups representing a range of locations and ages. We selected four cave lion and six modern lion individuals representing a range of locations and ages (expanded dataset), corresponding to (cave lions): East Asia (20 ka, "CE_Asia_20KYA"), Siberia (33 ka, "SiberiaA_33KYA"), New

Please cite this article in press as: Stanton et al., Paleogenomes reveal the evolutionary relationship between modern and cave lions, Cell (2026), https://doi.org/10.1016/j.cell.2026.05.007

Siberian Islands (52 ka, "NSI_52KYA"), Siberia (148 ka, "Siberia_148KYA") and (modern lions): Southwest Asia (Pleo_SouthwestAsia1, Pleo_SouthwestAsia2, Pleo_SouthwestAsia3), North Africa ("Pleo_Barbary1"), Central Africa ("Pleo_Sudan"), and South Africa ("Pleo_RSA"). We randomly searched trees with no admixture (plusminus_generations = 15, stop_gen = 200, stop_gen2 = 50) to identify the best supported topology. Three specimens from Southwest Asia were included, because the provenance of one of these, Pleo_SouthwestAsia2, was of suspected Southwest Asian origin, but this was not previously confirmed.[14] We then repeated the tree search after excluding Pleo_SouthwestAsia1&3, and allowing for n=1-2 admixture edges (num_admix = n; Figure S2).

Shared ancestry and admixture proportion calculations

We investigated shared genetic drift between all combinations of lions, using clouded leopard as an outgroup. We investigated which cave lion populations were closest to modern lions, and visa versa, using f4 statistics (carried out in popstats[73,74] on all permutations of cave lion ("Cave-X") and modern lion ("Lion-Y" and "Lion-Z"), with the formulations, f4(Clouded leopard, Cave-X; Lion-Y, Lion-Z), and f4(Clouded leopard, Modern-X; Cave-Y, Cave-Z) (Figures S3 and S4). This relationship was tested further using f4-ratios to estimate admixture proportion between different cave lion specimens and modern lions (Figure 3A). This test was carried out using the following setup: Pop1 (A in Patterson et al.[78]) = High Coverage Modern Southern Lion-A / Pop2 (O) = CloudedLeopard / Pop3 (X) CaveLion-X / Pop4 (C) = Old Cave Lion ("Siberia_148KYA") / Pop5 (B) = Modern Lion Source-B. In this setup, "High Coverage Southern Modern Lion-A" was all southern modern lion genomes with coverage >5X, and "CaveLion-X" and "Modern Lion Source-B" were all cave lion and modern northern lion genomes, respectively. Mean values were plotted against benthic 18O as a proxy for global ice extent[52] (Figure 3).

Cave lion genetic structure

In order to investigate broad patterns of genetic structure across space and time in cave lions, we calculated outgroup f3 statistics of the form f3(Recent cave lion, Cave X; Outgroup) (Figures S5A–S5C). To specifically investigate cave lion genetic structure between Siberia versus North America and Siberia versus Europe, we tested all combinations of f4 statistics of the form:

f4(Out, Cave-X[Eastern Eurasia]; Cave[N.America], Cave[Europe])

Where the North American sample was "Yukon_33KYA" and the European sample was "Austria_17KYA". To investigate the time-depth of genetic structure in North America, Europe and Central East Asia, we carried out f4 statistics of the form:

f4(Out, Cave[Siberia,Age-X]; Cave[Region=N.America/Europe/C.E.Asia], Cave[Recent Siberia])

This analysis made use of the non-Siberian genomes, to investigate if genetic structure existed between that location and Siberia, and if so, how old that genetic structure was. "Cave[Recent Siberia]" corresponded to a Siberian genome contemporary to the genome of interest: SiberiaA_33KYA for North America (Yukon_33KYA), Siberia_22KYA for Europe ("Austria_17KYA") and C.E.Asian ("CE_Asia_20KYA"), with "Cave[Age-X]" being all older Siberian genomes. A significant value (Z-score > 3) in this test is therefore evidence of "local ancestry" that predates the test genome ("Siberia, Age-X"), within the genome of interest ("Cave[Region=N.America/Europe/C.E.Asia]". If ancestry had been fully homogenised between Siberia and the region (Yukon/Europe/C.E.Asia) since the date of the older genome ("Siberia, Age-X"), we would expect this test to be non-significant (Figure S5D).

To investigate the magnitude of the persistent, local ancestry, we used a time series of Siberian genomes and an outgroup species (Clouded Leopard) within a qpAdm and qpWave framework. We first directly tested if a multi-source model was appropriate for North America and Europe using qpWave. In both cases, the "right" populations used were "Siberia_148KYA", "Siberia_64KYA", "NSI_52-KYA", "Siberia_47KYA", "Siberia_44KYA", "SiberiaA_33KYA", "SiberiaB_33KYA", "Siberia_30KYA", "CE_Asia_20KYA", and "Clouded leopard". The "left" populations used were "Austria_17KYA" and "Siberia_22KYA" to test the number of migrations into Europe, and "Yukon_33KYA" and "Siberia_22KYA" to test the number of migrations into North America. Both models were able to strongly reject a hypothesis of a single ancestry source ($p = 6.8e^{-07}$ and $p = 5.9e^{-52}$, respectively).

To investigate the presence and magnitude of "deep ancestry" that predates any local cave lion genetic structure, we used qpAdm on the European ("Austria_17KYA"), C.E. Asian ("CE_Asia_20KYA") and North American ("Yukon_33KYA") targets, with left (European and C.E. Asian) = "Siberia_22KYA" & Leopard (outgroup) and left (North American) = "SiberiaA_33KYA" & Leopard (outgroup); right (European and C.E. Asian) = Clouded leopard, Siberia_148KYA, Siberia_64KYA, NSI_52KYA, Siberia_47KYA, Siberia_44KYA, SiberiaA_33KYA, SiberiaB_33KYA, Yukon_33KYA, Siberia_30KYA and right (North American) = CloudedLeopard, Siberia_148KYA, Siberia_64KYA, NSI_52KYA, Siberia_47KYA, Siberia_44KYA. These were designed to use all available genomes in the right populations prior to the time of the target genome, with Clouded leopard included to polarise allele frequencies. Leopard was used as a proxy for deep ancestry that predates all lion genomes.

Timing ancestry homogenisation in cave lions

In order to investigate the timescale over which this Eurasian-wide homogenisation occurred, we carried out f4 statistics of the form:

f4(Outgroup,Cave-X;Siberia_Young1,Siberia_Old1)

f4(Outgroup,Cave-X;CE_Asia_Young2,Siberia_Old2)

Please cite this article in press as: Stanton et al., Paleogenomes reveal the evolutionary relationship between modern and cave lions, Cell (2026), https://doi.org/10.1016/j.cell.2026.05.007

This setup tests for the timing of population connectivity. If Cave-X had been completely isolated from Siberia between the period Siberia_Young1 to Siberia_Old1, we would expect it to be symmetrically related to the old and young genomes in the test. Conversely, more shared drift with the younger Siberian genome would demonstrate gene-flow between Siberia and Cave-X during this time period. In the same way, additional shared drift over a younger time period (Young2 to Old2) demonstrates additional gene-flow event(s) (Figure S5E).

Admixture graphs

To verify and summarise the genetic structure results, we constructed an admixture graph using a subset of the above cave lion genomes (covering the main timescale/regions sampled). We ran the find_graphs function in AdmixTools2 (plusminus_generations = 15, stop_gen = 200, stop_gen2 = 50), with both 0 and 1 admixture edge. We then iteratively added admixture edges on to the ''1-admixture-edge'' graph with the lowest score, using the graph_plusone function. We concluded that the graph with $n = 2$ admixture edges was the most appropriate (Figure S5H). Notably, the admixture edge for the European sample originates from a relatively much less deep position than for the North American sample in the admixture graph. The estimates of genetic drift along these graph edges indicates that the deep ancestry detected in the European genome occurs relatively close to the sampled, cave lion diversity: Approximately 8% along the branch between the ancestor of ''Siberia_148KYA'' and the common ancestor of lions and clouded leopards (10/[10+58+55] = 0.08), likely placing this ancestry within, or very close to, the overall cave lion diversity. The deep ancestry detected in the North American individual originates from a point over 50% along the branch between our sampled cave lion diversity and the split between cave lions and clouded leopards ([10+58]/[10+58+55] = 0.55). However, a caveat to this is that because the deep ancestries in the model originate from unsampled populations, the admixture fraction and the point of divergence are confounded with each other and therefore not necessarily well-constrained: there might be many possible combinations of admixture fractions and divergence points that all would be compatible with the data.

To compare the fits of these graphs, we 1. Carried out an out of sample adjustment and bootstrap resampling (as per ''out-of-sample-adjustments''[79]). One, two, and three admixture edges were a significantly better fit than zero admixture edges ($p = 0.027$, $p = 0.020$, $p = 0.007$), but none of the graphs with admixture edges were a significantly better fit than any of the others ($p > 0.05$). Confidence intervals were calculated using the qpgraph_resample_snps function. We also assessed the fit of the admixture graphs by, 2. Extracting the worst residual, and the number of z-scores from the f4 comparisons that are $|z| > 3$. The worst residual for the $n = 0$, 1, 2 & 3 admixture edges was 13.13, 7.18, 5.58 and 5.58, respectively. Finally we, 3. Identified the number of z-scores where $-3 > z > 3$ for the same set of graphs, above. The number of z-scores outside of the range $-3 > z > 3$, for the one, two, and three admixture edge graphs was 9.93% (201 of 2025 comparisons), 4.15% (84 of 2025 comparisons), 1.68% (34 of 2025), and 1.58% (32 of 2025), respectively.

Based on the graphs with admixture edges being a better fit than the one without (test 1, above), and due to the residuals being a better fit until $n = 2$ admixture edges, but not beyond that (tests 2 & 3, above), we conclude that the graph with $n = 2$ admixture edges was the most appropriate (Figure S5H).

Demographic inference

We investigated changes in effective population size using PSMC, on representatives of four modern lion populations (Southwest Asian, ''Pleo_SouthwestAsia2''; Barbary, ''Pleo_Barbary1''; South Africa, ''Pleo_RSA''), and the one high coverage cave lion genome (''CE_Asia_20KYA''). Reads were re-mapped to the lion genome[80] using the same settings as above for the cat genome. We called variants using bcftools v1.8[63] and converted the VCF file to a consensus fastq using vcfutils,[62] excluding sites with coverage <1/3X or >2X the genome-wide mean coverage. We then converted the consensus fastq to a PSMC fasta, and ran PSMC with 100 bootstrap replicates, a lion generation time of 5 years and a mutation rate of 4.5e-9 as per de Manuel et al.,[14] using PSMC.[81] The timescale for the cave lion was adjusted to reflect its ^{14}C age (19,782 ybp).

Lion divergence times

There is considerable variation in estimates of divergence time between modern and cave lions when considering nuclear genomes only,[14] and based on mitochondrial genomes and fossil constraints.[16,17] Given that admixture is known to complicate divergence time estimates in other felids,[19] we hypothesise that shared ancestry between modern and cave lion lineages is lowering this previous nuclear-based divergence time estimate. Different levels of gene-flow at different time points (Figure 3) would imply that multiple combinations of divergence time and gene-flow estimates may be consistent with the empirical data, however assuming reciprocal monophyly (Figures 1B and S2), the correct divergence could be inferred by identifying where the highest density of viable parameter combinations occur.

We used this approach in an attempt to constrain the divergence time estimate, using simulations carried out in msprime (v1.2.0)[66] using a range of divergence times and rates of migration between modern and cave lions. $F(A_{derived}|B_{heterozygous})$ statistics[82] were then estimated for each of these parameters, for multiple modern and cave lion combinations, and compared to empirical estimates of F(A|B). For these models, we assumed a split of an ancestral lion lineage split from an outgroup 6.19 MYA,[49] before splitting into modern and cave lion lineages 0.25, 0.5, 0.75, 1, 1.25, 1.5, 1.75 and 2 ma. A split between a North and South cave lion populations (of equal effective population size) 200 ka (to predate the oldest cave lion genome), and a split between North and South modern lion lineages 70 ka.[14] To account for the high level of ancestry connectivity within cave lions, we modelled continuous gene-flow from the

Please cite this article in press as: Stanton et al., Paleogenomes reveal the evolutionary relationship between modern and cave lions, Cell (2026), https://doi.org/10.1016/j.cell.2026.05.007

North to the South population (rate = 0.9). We included bi-directional gene-flow between the southern cave lion and northern modern lion populations, at rates of between $1.0e^{-6}$ to $3.0e^{-5}$, in steps of $1.0e^{-6}$ (total of 30 steps). We modelled this (modern/cave) gene-flow as "pulses", occurring 100 years before each sampled cave lion genome, lasting for 1 generation, to reflect our finding that introgression rate appears to vary over time. A generation time of five years was used[14] and estimates of effective population size were taken from the above PSMC analysis. F(A|B) values were calculated for both simulated and empirical data, using popstats,[73] and alpha (ancestry proportion) calculated for the simulated data in the same way as for the empirical data (f4 ratios, above). We then identified viable combinations of divergence time and migration rate as those where simulations overlapped with empirical estimates.

Partitioning of variation and identification of positive selection

Filtered VCF files were generated as for those in "*Variant calling and ascertainment panel*", above, except that all sites were included rather than just variable positions. The pseudohaploid allele calls for lions were then added to this VCF of all sites. To investigate how variation was partitioned across our dataset we filtered the VCF file to exclude sites with missing data at >50% of individuals within any of the following groups: Outgroups, modern lions, and cave lions. We then extracted and counted all combinations of the following conditions within each of those groups, using bcftools v1.8[63]: Fixed for reference allele, fixed for alternate allele, variable for reference/alternate. We identified all variable positions that were either classified as synonymous or non-synonymous, using SnpEff,[56,57] and carried out a McDonald-Kreitman test[55] for positive selection across the cave lion genome. We then identified "high" impact mutations (using SnpEff[56,57]; loss of function or severe disruption of the gene) that were fixed in, and unique to the cave lion lineage (relative to the domestic cat, all six outgroups, and modern lions). Finally, we investigated genes with an excess of *de novo* non-synonymous mutations in cave lions (i.e. as above, but not limited to fixed variation), relative to the expectation based on alleles polymorphic across modern and cave lions. This test thereby identifies cave lion genes with an excess of unique non-synonymous mutations. Those genes with the best evidence for an excess of unique non-synonymous mutations (lowest 1% of p-values with denovo_N:denovo_S ratio > P_N:P_S ratio; n = 124, $p = 3.1e^{-4}$ - $3.8e^{-16}$) were included in a Gene Ontology enrichment test using GO (Figure 6).[58,59]

Supplemental figures

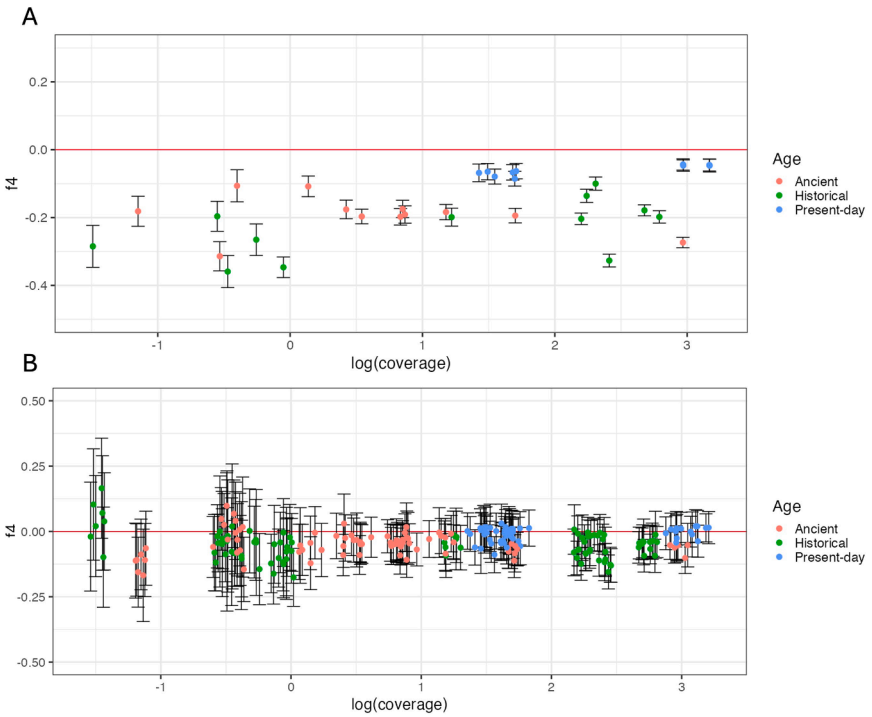

Figure S1. f4 tests to investigate the extent of reference bias in the full SNP dataset, related to STAR Methods

These values were calculated as: f4(outgroup, Lion X, Reference, cat), with reference bias appearing as gene flow between Lion X and the reference, in the form of significant negative values. Whiskers correspond to three SEs and colors correspond to sample type.

(A) Loci were ascertained in all lion individuals with no outgroup ascertainment, and leopard (*P. pardus*) used as the outgroup for the f4 statistic. Consistent significant negative values and large variation between sample types signify considerable reference bias.

(B) Loci were ascertained in the following six outgroup taxa: Bengal tiger (*P. tigris*), clouded leopard (*Neofelis nebulosa*), leopard (*P. pardus*), jaguar (*P. onca*), Siberian tiger (*P. tigris*), snow leopard (*P. uncia*), in one high- coverage modern lion sample (*Panthera leo*, Central Africa), and the ancient high-coverage cave lion ("CE_Asia_20KYA," Central East Asia). All six outgroup taxa were tested as the outgroup for the f4 test, with points jittered on the *x* -axis. The shift of values towards zero, and no obvious variation between sample types, suggests no systematic reference bias.

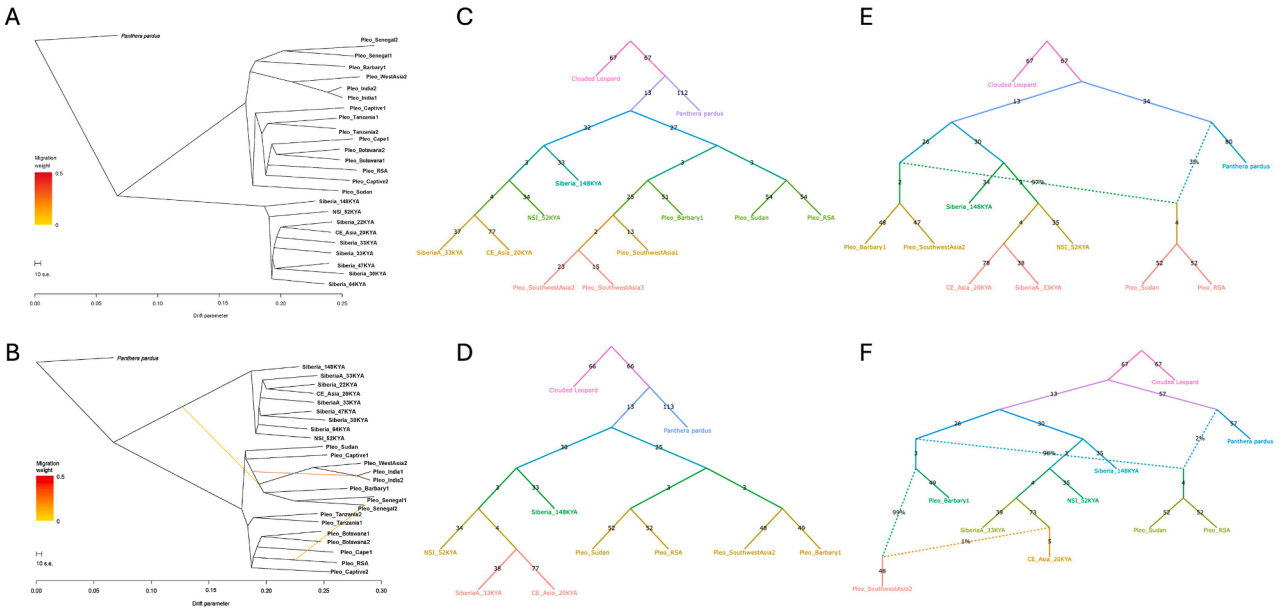

Figure S2. TreeMix phylogeny and admixture graphs to investigate lion population structure, related to STAR Methods

TreeMix phylogeny of lions and cave lions, related to Star Methods, with (A) 0 and (B) 3 migration edges. The optimal number of migration edges (m) was determined to be three (tested 0–10 edges, with 10 repeats for each), based on the second-order rate of change in likelihood (Δm).[83] Low coverage (<1×X) individuals, and sites with missing data, were excluded.

(C–F) Admixture graphs to investigate topology and gene flow in modern and cave lions. (C) Two low-coverage Mesopotamian lions were included to investigate the placement of the "Pleo_SouthwestAsia2" specimen. (D–F) Best-supported admixture graphs (excluding samples "Pleo_SouthwestAsia1" and "Pleo_SouthwestAsia3"), including 0–2 admixture edges, respectively. The graph with two admixture edges has the highest likelihood, although after computing out-of-sample scores and bootstrapping resampled SNP blocks,[77,79] neither model with admixture was a significantly better fit than the corresponding one with $n-1$ admixture edges (0 vs. 1, p = 0.280; 1 vs. 2, p = 0.127).

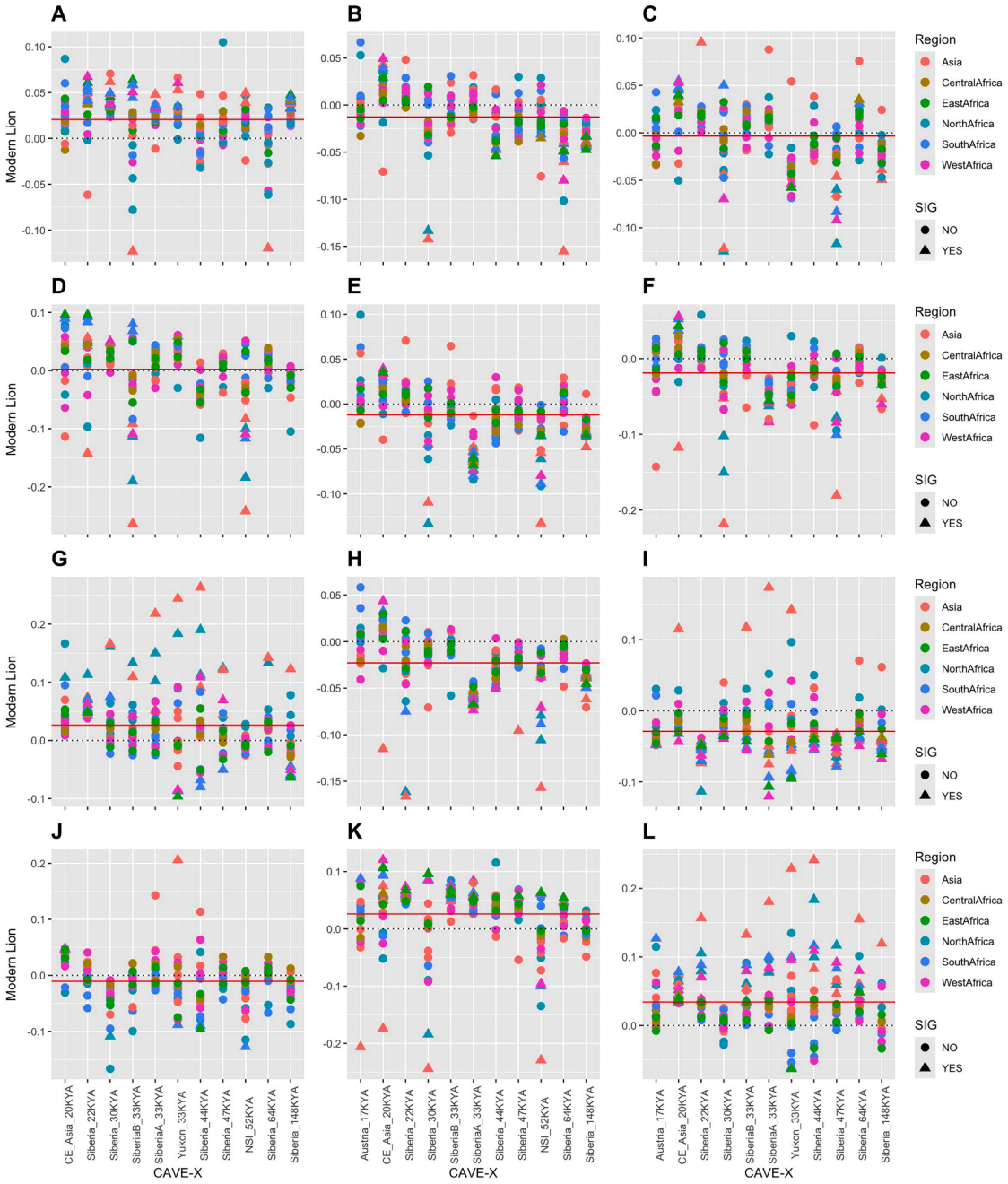

Figure S3. f4 tests to explore potential asymmetries in modern lion ancestry within different cave lion genomes, using the formulation f4(Clouded leopard, Modern Lion; Cave-Y, Cave-X), related to Figures 3 and 4

The horizontal red line shows the mean f4 value, and *Z* scores less than −3 or greater than 3 are shown as triangles. All combinations of Modern Lion and Cave-X were carried out, with Cave-Y being kept constant per plot (A–L);, values greater than zero (horizontal black dashed line) indicate that the modern lion (colored by region) is closer to Cave-X (*x* axis) than Cave-Y (plot title).

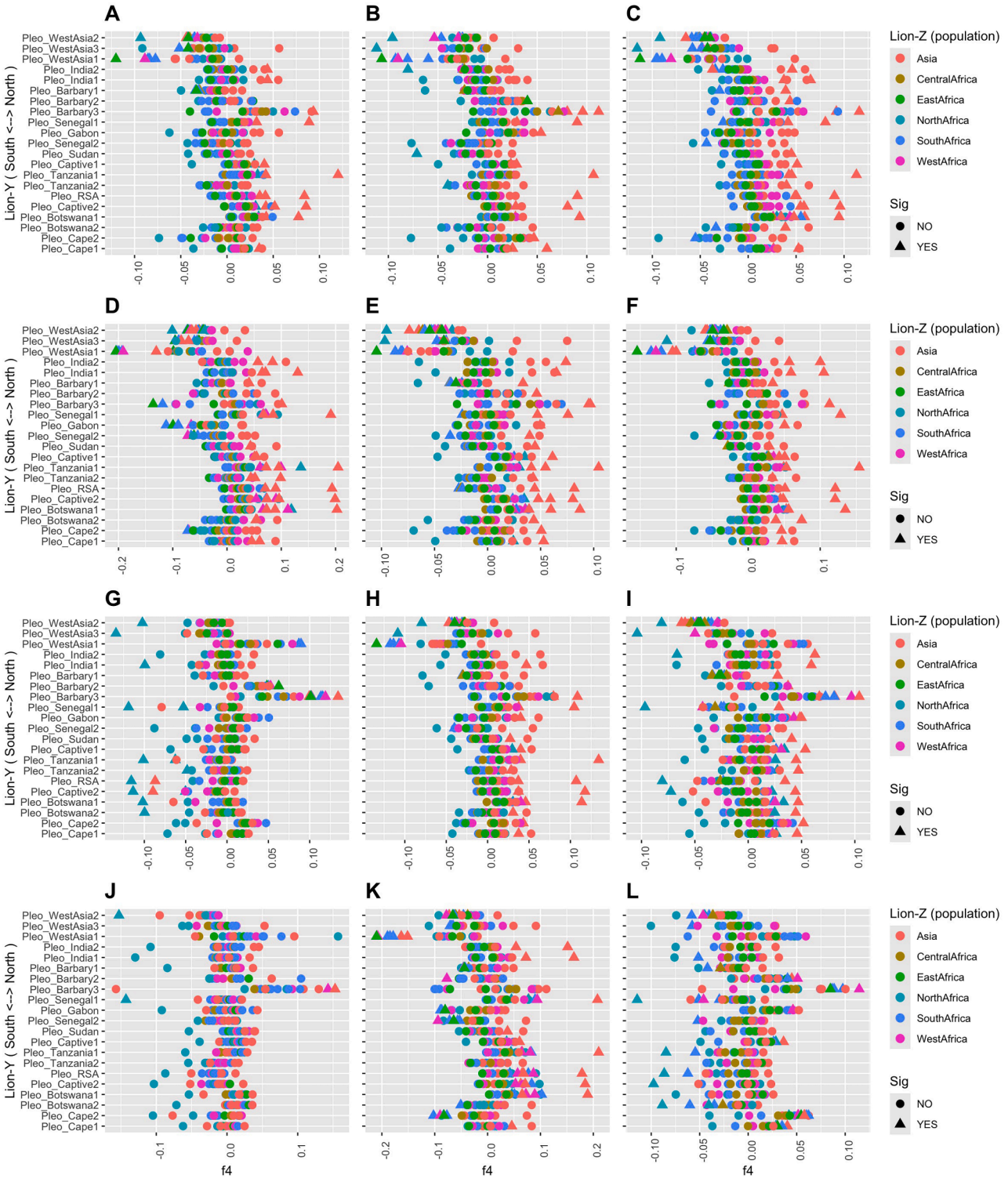

Figure S4. f4 tests to investigate asymmetries in ancestry between the modern lions and each of the cave lion samples, using the formulation f4(Clouded leopard, Cave-X; Lion-Y, Lion-Z), related to Figure 4

All combinations of Cave-X and Lion-Y and Lion-Z were carried out (A–L), with Cave-X given in the title of each plot. The top three modern lions on the *x* -axis on each plot correspond to the individuals from the extinct Southwest Asian population (Pleo_SouthwestAsia1–3).

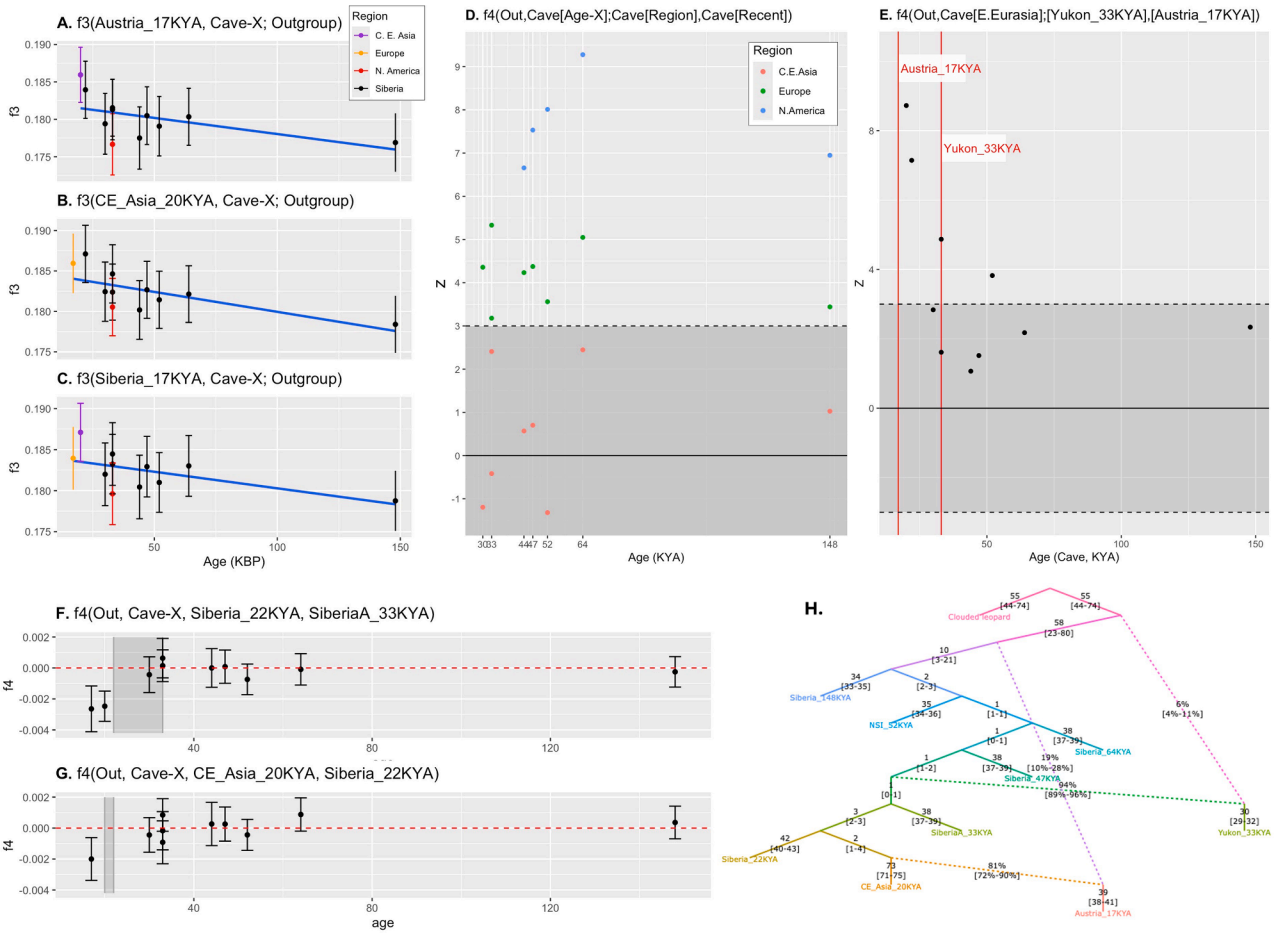

Figure S5. Shared genetic drift and homogenization of ancestry over time, related to Figure 2

(A–C) Shared genetic drift in cave lions over time, calculated as f3(Recent cave lion, Cave-X; Outgroup), with the "recent cave lion" corresponding to an individuals from Europe (A), C.E. Asia (B), and Siberia (C). The sample from North America ("Yukon_33KYA") is shown in red, and consistently shows less shared genetic drift than other contemporary individuals, especially when compared with the European specimen ("Austria_17KYA"). Whiskers show three standard errorSEs.

(D) f4 statistics of the form f4(Out, Cave[Siberia, Age-X]; Cave[Region = N.America/Europe/C.E.Asia], Cave[Recent Siberia]). In this test, a significant (z > 3) result demonstrates persistent genetic structure in the cave lion from the region listed, with the age of "Cave[Siberia, Age-X]" indicating the age of that structure.

(E) f4 statistics of the form f4(Out, Cave-X[Eastern Eurasia]; Cave[N.America], Cave[Europe]), with significant positive values (z > 3) consistently demonstrating affinity between Eastern Eurasia and Europe, relative to Eastern Eurasia and North America.

(F and G) f4 statistics testing the timescale of homogenization of ancestry across Eurasia. (F) f4 tests for two Siberian cave lions over the period of 22–33 ka, against all other cave lion individuals: f4(Outgroup, Cave-X; Siberia_22KYA, Siberia_33KYA). (G) f4 tests for a 20 ka and 22 ka cave lion from C.E. Asia and Siberia, respectively, against all other cave lion individuals: f4(Outgroup, Cave-X; CE_Asia_20KYA, Siberia_22KYA).

(H) Admixture graph with two admixture edges, based on comparison between graphs using out- of- sample scores and bootstrapping, the value for the worst residual, and the number of residuals for which f4 values |z| > 3. Percentages show the relative proportions of admixture, and the whole numbers in parentheses show the range of predicted drift along each admixture edge.